

**IN SITU ALUMINIUM COMPOSITES**

**A DISSERTATION**

**Submitted in partial fulfillment of the  
requirements for the award of the degree**

**of**

**MASTER OF TECHNOLOGY**

**in**

**METALLURGICAL AND MATERIALS ENGINEERING**

**(With Specialization in Industrial Metallurgy)**

**By**

**MAYANK THAPLIYAL**

**(Enrolment No: 16544008)**



**DEPARTMENT OF METALLURGICAL AND MATERIALS ENGINEERING**

**INDIAN INSTITUTE OF TECHNOLOGY ROORKEE**

**ROORKEE – 247667 (INDIA)**

**MAY-2018**

## CANDIDATE'S DECLARATION

---

I hereby declare that the proposed work presented in this dissertation entitled **IN SITU ALUMINIUM COMPOSITES** in partial fulfillment of the requirements for the award of the degree of **Master of Technology in Metallurgical and Materials Engineering** with specialization in **Industrial Metallurgy** submitted in the **Department of Metallurgical and Materials Engineering, Indian Institute of Technology Roorkee** is an authentic record of my own work carried out during the period from July 2016 to May 2018, under the supervision of **Dr. B.S.S. DANIEL** Professor, Department of Metallurgical and Material Engineering, Indian Institute of Technology Roorkee.

The matter presented in this dissertation has not been submitted anywhere in any form by me for awarding any degree.

**Dated:**

**Place: Roorkee**

**(MAYANK THAPLIYAL)**

---

### CERTIFICATE

This is to certify that the above statement made by the candidate is correct to the best of my knowledge and belief.

**(Dr. B.S.S. DANIEL)**

Professor

Department of Metallurgical & Materials Engineering

Indian Institute of Technology Roorkee

Roorkee-247667 (INDIA)

## ACKNOWLEDGEMENT

I would like to thank the almighty God for his protection and giving me peace throughout my work. I am highly indebted to **Dr. B.S.S. DANIEL**, Professor, Department of Metallurgical and Materials Engineering, Indian Institute of Technology Roorkee, for encouraging me to undertake this dissertation as well as providing me all the necessary guidance and inspirational support throughout this dissertation work. He has displayed unique tolerance and understanding at every step of progress. It is my proud privilege to have carried out this dissertation work under his valuable guidance.

I wish to express my sincere thanks to **Dr. Anjan Sil**, Professor and Head of the Department, Metallurgical and Materials Engineering Department, Indian Institute of Technology Roorkee, for his help to carry out this dissertation. I would also thank each and every staff members involved in carrying out my experiments successfully.

I also like to express my gratitude to Research Scholars for their innumerable discussion and generosity and willingness to share their knowledge. I sincerely appreciate their valuable guidance and persistent encouragement in making this work.

I would like to acknowledge all friends for their valuable information and developing love and confidence in me throughout the work. Last but not the least I would like to thanks my parents who supported me morally to accomplish this task to an achievable one.

Date:

(MAYANK THAPLIYAL)

M-Tech  
Industrial Metallurgy

---

## **ABSTRACT**

Preparing aluminum matrix composites (AMCs) using in situ method results in many desirable benefits. Here it is focused on preparing AA6061/ (0%, 3% by simple casting method, 3% with ultrasonication, 6% by simple casting method, 6% with ultrasonication ZrB<sub>2</sub> AMCs by Al–K<sub>2</sub>ZrF<sub>6</sub>–KBF<sub>4</sub> reaction system. The inorganic salts were added to molten aluminium alloy at an elevated temperature of 850°C. The prepared AMCs were studied by applying conventional microcopy and advanced characterization techniques. XRD peaks confirmed the successful synthesise of ZrB<sub>2</sub> particles. No other phases such as Al<sub>3</sub>Zr and AlB<sub>2</sub> were detected in appreciable quantity. There was a refinement of grains in the composite due to ZrB<sub>2</sub> particles. Two kind of distribution was observed in the micrographs. Particle clusters were observed with increased weight fraction of particles. ZrB<sub>2</sub> particles were observed to be sub–micron and nano level in size and characterized by proper interfacial bonding with the aluminum matrix. The mechanical properties were improved remarkably by the incorporation of ZrB<sub>2</sub> particles and the possible strengthening mechanisms were discussed.

## **TABLE OF CONTENTS**

Title page.....	i
Candidate's Declaration.....	ii
Acknowledgement.....	iii
Contents .....	IV
Abstract.....	v
List of figures.....	vi
List of tables.....	viii
List of Abbreviations.....	ix

### **CHAPTER1: INTRODUCTION**

1. Introduction.....	1
1.1 In Situ Composites.....	2
1.2 Intermetallic Matrix Compound.....	2
1.3 Effect of Ultrasonication.....	3
1.4 Tensile Strength and Yield Strength.....	4
1.5 Fracture Toughness.....	4
1.6 Flexural Strength.....	5
1.7 Flexural v/s Tensile Strength.....	6
1.8 Hardness.....	8

### **CHAPTER 2: LITERATURE SURVEY.....11**

### **CHAPTER 3: PLAN OF WORK..... 19**

**CHAPTER 4: EXPERIMENTAL PROCEDUERE.....22**

**CHAPTER 5: RESULTS AND DISCUSSIONS.....23**

**5.1 XRD Analysis.....23**

**5.2 Microstructure Study.....24**

**5.3. Tensile Test.....26**

**5.4 Hardness.....28**

**5.5 Flexural Strength.....30**

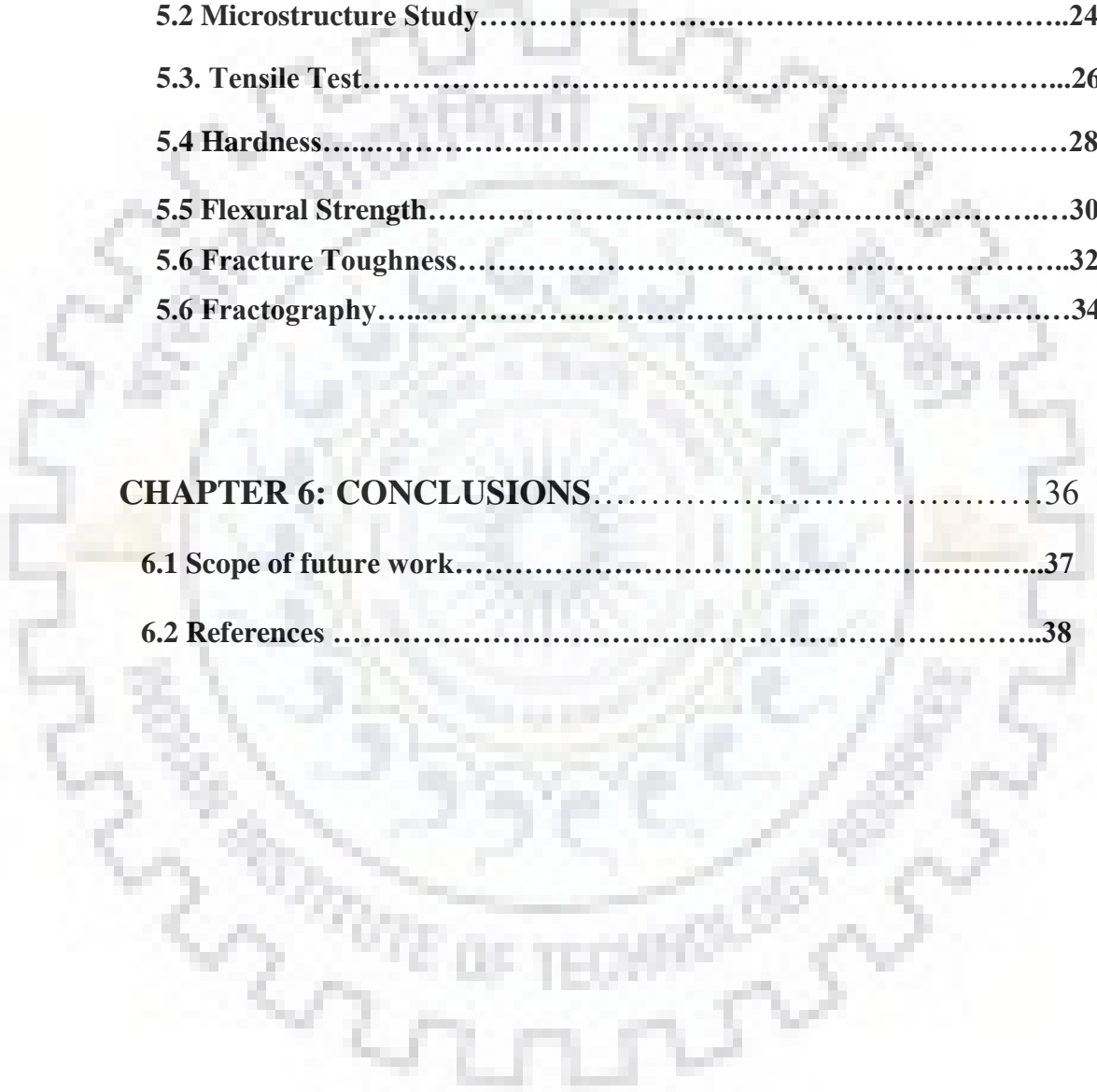
**5.6 Fracture Toughness.....32**

**5.6 Fractography.....34**

**CHAPTER 6: CONCLUSIONS .....36**

**6.1 Scope of future work.....37**

**6.2 References .....38**



## LIST OF FIGURES

<b>Fig. No.</b>	<b>Description</b>	<b>Page No.</b>
<b>Fig. 1</b>	Sketch of effects of ultrasonic cavitation and acoustic streaming on particles distribution.	<b>4</b>
<b>Fig. 2</b>	Flexural stress is the Stress at failure.	<b>5</b>
<b>Fig. 3</b>	Beam of material under bending. Extreme fibers at B (compression) and (tension)	<b>6</b>
<b>Fig. 4</b>	Stress distribution across beam.	<b>6</b>
<b>Fig. 5</b>	Beam under 3 point bending.	<b>7</b>
<b>Fig. 6</b>	Optical micrographs of AA2024/ZrB <sub>2</sub> in situ composites containing ZrB <sub>2</sub> : (a) 0 wt%, (b) 3wt%, (c) 3 wt % with ultrasonication (d) 6 wt% and (e) 6 wt% with ultrasonication..	<b>18</b>
<b>Fig. 7</b>	Experimental setup with ultrasonic transducer.	<b>21</b>
<b>Fig. 8</b>	.Schematic diagram of ultrasonic assisted casting.	<b>21</b>
<b>Fig. 9</b>	XRD patterns of the fabricated composites and base Al alloy.	<b>22</b>
<b>Fig. 10</b>	10 SEM micrographs of AA6061/ZrB <sub>2</sub> in situ composites containing ZrB <sub>2</sub> : (a) 3 wt%, (b) 3 wt% with ultrasonication(c) 6 wt% and (d) 6 wt% with ultrasonication..	<b>25</b>

<b>Fig. 11</b>	Engineering stress-engineering strain curves of base Al alloy and composites.	<b>27</b>
<b>Fig. 12</b>	Variation in hardness of base Al alloy and the developed composites.	<b>29</b>
<b>Fig. 13</b>	Flexural Stress-Strain curve of base Al alloy and the developed composites.	<b>31</b>
<b>Fig. 14</b>	Variation in Fracture Toughness of composites.	<b>33</b>
<b>Fig15</b>	SEM micrograph of the fracture surface of tensile specimens (a) base Al alloy; (b) 3wt% ZrB <sub>2</sub> (c) 6 wt% ZrB <sub>2</sub> .(d) 6 wt% ZrB <sub>2</sub> with ultrasonication	<b>35</b>



## LIST OF TABLES

<b>Table No.</b>	<b>Description</b>	<b>Page No.</b>
<b>Table 1</b>	Chemical composition of Al6061 alloy.	<b>19</b>
<b>Table 2</b>	Samples and their Compositions	<b>22</b>
<b>Table 3</b>	UTSs, Elongations and %Increases	<b>28</b>
<b>Table 4</b>	Flexural Strength and Strain values	<b>30</b>
<b>Table 5</b>	Values of Fracture Toughness	<b>32</b>

## **LIST OF ABBREVIATIONS**

AMCs-ALUMINIUM MATRIX COMPOSITES.

IMCs-INTERMETALLIC MATRIX COMPOUNDS

IC-INTERMETALLIC COMPOUNDS

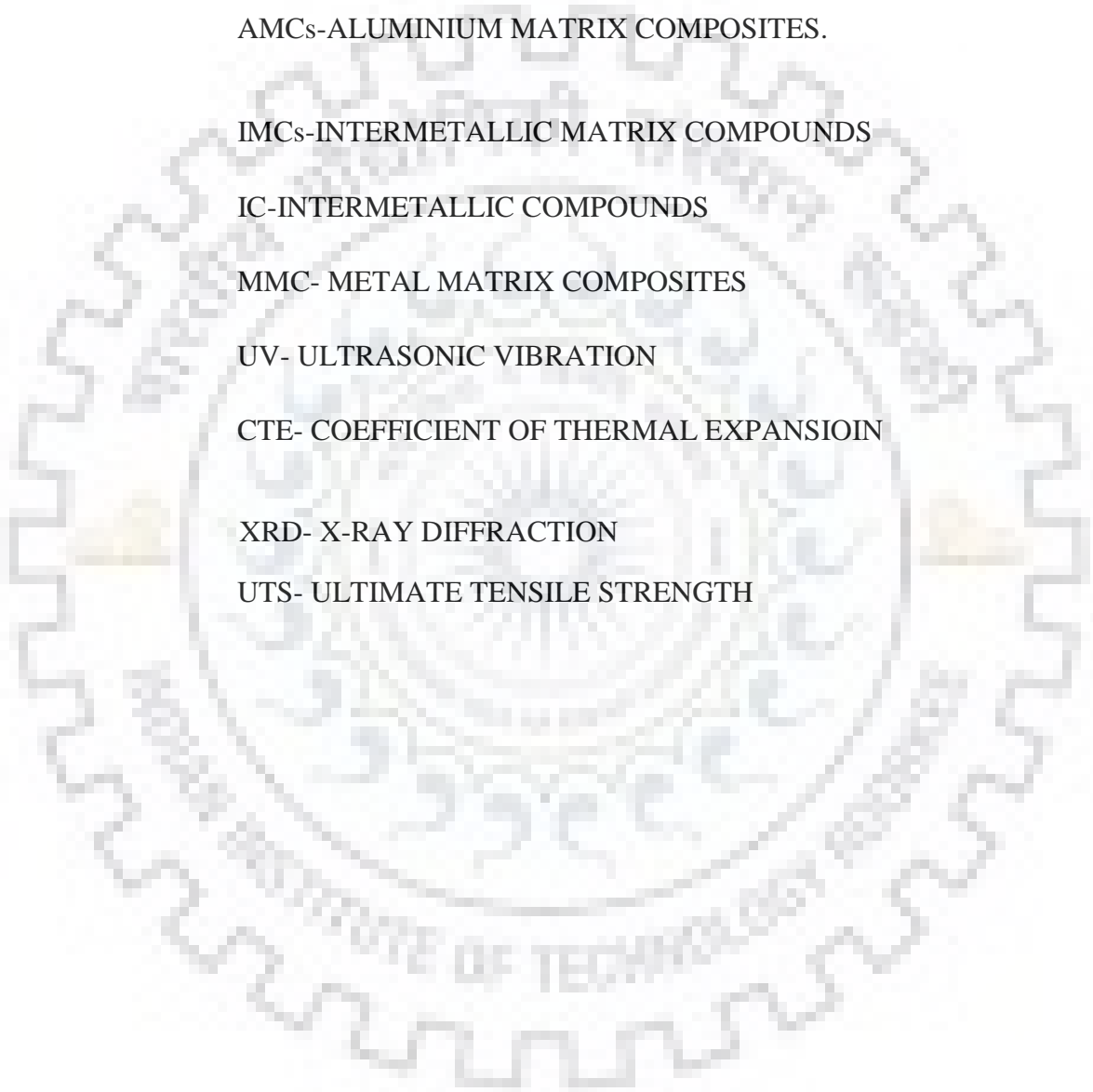
MMC- METAL MATRIX COMPOSITES

UV- ULTRASONIC VIBRATION

CTE- COEFFICIENT OF THERMAL EXPANSIOIN

XRD- X-RAY DIFFRACTION

UTS- ULTIMATE TENSILE STRENGTH





## **1. Introduction**

The ever increasing demand for light weight and high performance materials lead to the invention and development of aluminum matrix composites (AMCs). The requirement for high specific strength, superior wear resistance and stability at elevated temperature are satisfied by AMCs. Conventional aluminium composites are slowly phased out in several industrial applications due to the superior service performance of AMCs. It remained as a tradition to use SiC and Al<sub>2</sub>O<sub>3</sub> particles as reinforcement phase for AMCs due to low cost and superior wettability with molten aluminum. The improvement and discovery of new manufacturing processes showed the way to reinforce other potential ceramic and various kinds of particles to produce AMCs. ZrB<sub>2</sub> particles have drawn the attention to reinforce AMCs apart from much researched boride particle accumulating roll bonding have been developed as potential solid state methods for producing AMCs. Nevertheless, it is impossible to produce a complex shape or desired ZrB<sub>2</sub>. ZrB<sub>2</sub> particles are characterized by higher hardness, very high melting point, thermal; stability and excellent resistance to wear. ZrB<sub>2</sub> is a good conductor of heat and electricity.

Although a spectrum of techniques is available to produce AMCs, it is not possible to reinforce every kind of reinforcing particulate with the aluminum matrix. Commonly employed techniques are powder metallurgy and stir casting. Recently, friction stir processing and component shape using those techniques. Liquid metallurgy routes i.e. metallic matrix is completely melted during the process are applied widely for industrial products. The main reasons are lesser production cost, adoptability for mass production and absence of complex procedure. The popular method stir casting poses huge challenge due to deprived wettability of reinforcing particles with molten aluminum, weak interfacial bonding and likelihood of reaction between the ceramic particle and the aluminum matrix. Those issues can be overcome if reinforcing particles are synthesized within the molten aluminum. This technique was called as in-situ method which gained popularity in the last decade. The features of this method are thermodynamically stable particles, smaller size particles, superior interfacial bonding and improved wettability. It was demonstrated in literatures to develop AMCs reinforced with in-situ formed Al<sub>2</sub>O<sub>3</sub>, TiC, TiB<sub>2</sub>, ZrB<sub>2</sub> particulates.

This work is focused on preparing AA6061/ZrB<sub>2</sub> AMCs via reaction system Al–K<sub>2</sub>ZrF<sub>6</sub>–KBF<sub>4</sub>. Advanced characterization techniques were employed to characterize the developed composite.

In the present work,  $K_2ZrF_6$ – $KBF_4$  inorganic salt was added into the Al melt to form in-situ  $ZrB_2$  particles. Ultrasonication was applied for better distribution of salt particles throughout the molten metal. It is well known that better distribution of in-situ particles along with limited porosity will improve the mechanical properties of the composite. Therefore, an attempt is made to fabricate  $ZrB_2$  reinforced aluminium matrix composite using low cost salt-metal reaction route.

### **1.1. In situ composite**

'In situ composite' is the term applied to a relatively small, but fast expanding domain of materials where the reinforcing phase is formed within the parent phase by controlled melt growth, chemical reaction, transformation and deformation. This single stage process has considerable advantages over conventional synthetic composites as it avoids complicated additional steps such as sorting, alignment, infiltration and sintering. Hence these processes are cost effective. The interfaces produced are relatively stable and impurity-free. Additionally, the strength of selected in situ composites is better than conventional materials. This in situ concept is not entirely new, as nature provides many examples such as wood, bone etc. But, man-made in situ composite manufacturing is confined to the thermodynamic and kinetic space, through control of composition and process variables to arrive at the desired duplex structures. But today, in situ composites consist of metals, intermetallic, ceramics and organic compounds whose microstructural control led to new avenues in magnetic, electrical, optical, thermal, chemical and structural applications.

### **1.2. Intermetallic matrix composites (IMCs)**

Intermetallic matrix composites (IMCs) are distinguished from metal matrix composites (MMCs) by the fact that the matrix is an ordered intermetallic compound or a multiphase combination of intermetallic compounds. In some cases, materials that possess a significant fraction of an ordered intermetallic compound (IC), or where the IC is the reinforcement, have also been referred to as intermetallic composites. As a distinct class of materials, IMCs have their origins in the two disciplines of MMCs and ordered intermetallic compounds and alloys. A major objective of each of these two activities has been to develop structural aerospace materials for use at elevated temperatures, and IMCs are a product of collaboration between these parallel efforts.

ICs also often possess a lower density than other candidate high-temperature structural alloys. However, ICs typically suffer from inadequate fracture properties, with unacceptably low tensile

strains to failure and fracture toughness as a rule. In addition, single-phase intermetallic alloys often have poor creep resistance at projected use temperatures. Thus, the IC technical community has pursued the addition of a reinforcing phase to improve the high-temperature creep response through a load-sharing mechanism with the (generally ceramic) reinforcement. Reinforcements have also been incorporated to increase the fracture resistance of ICs. Along with the concepts of crack deflection and crack bridging, ductile “reinforcements” and novel composite architectures, such as co-continuous networks of interpenetrating phases and micro laminated composites, have been considered to increase fracture resistance.

The addition of a reinforcing phase to a metal alloy typically improves strength and stiffness, but the high-temperature response of an MMC is still limited by the basic characteristics of the metal matrix. This is especially true for discontinuously reinforced MMCs, but is also true for continuously reinforced MMCs, since multi axial loading is nearly always a requirement for real components. In order to improve the elevated temperature properties of MMCs, intermetallic matrices have been substituted for conventional (i.e., disordered) metal matrices. In many cases, the IC has the added benefit of reduced reaction kinetics with the reinforcing phase.

### **1.3. Effects of the Ultrasonication**

The improvements of particles distribution of AA6061/ZrB<sub>2</sub> AMCs composites can be explained by the effects of the ultrasonic cavitation and the acoustic streaming. The cavitation generates high pressure shock-waves and the shock-waves impact the aggregates. When large aggregates are impacted by shock-waves, the weak bonded part of large aggregates is directly broken into dispersed particles and the well bonded part is broken into small ones. The acoustic streaming also works at the same time. The whirlpools caused by the acoustic streaming are continuously homogenizing the melt. So the whirlpools can uniform the particles distribution in the melt and continuously bring the large aggregates to the area where the cavitation intensely works. Therefore the breaking of large aggregates becomes very effective with the combination work of the ultrasonic cavitation and the acoustic streaming, and large aggregates are eliminated with a short time UV treatment for just 30 s. When the large aggregates are eliminated, there are only small aggregates which is well bonded left in the melt. These well bonded small aggregates also can be broken by the repeated impacts of shock-waves. Since the cavitation is mainly effectively working in region under ultrasonic vibration generator, it takes 120 s for the UV treatment to eliminate all the small aggregates. After the elimination of all the aggregates, The processing of

the elimination of the aggregates and the homogenization of the particles distribution can be summarized to a sketch as shown in Fig. 1 shows the the particles are uniformly distributed through the bulk melt. So the gathering of particles at grain boundary regions is refined and becomes more uniform through the bulk matrix after solidification average grain size of base metal and AA6061/ZrB<sub>2</sub> AMCs composites either treated by UV or untreated.

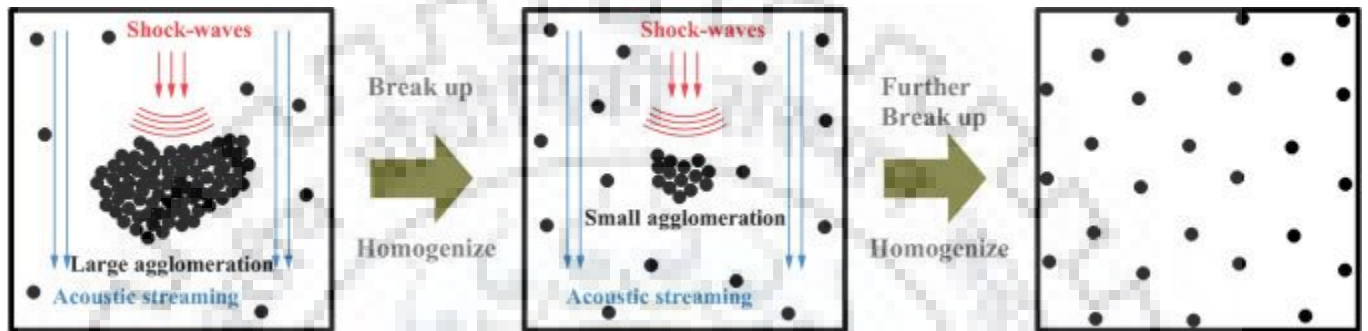


**Fig 1 Sketch of effects of ultrasonic cavitation and acoustic streaming on particles distribution.**

#### **1.4. Tensile Strength and Yield Strength**

Tensile strength, or breaking strength, is one of the major attributes of a material. It is a measure of the degree of coherence of a material, and without it, other properties have little importance.

Tensile strength is the breaking strength of a specimen under exertion of a force capable of breaking many threads simultaneously, at a constant rate of extension/ load. It may be more readily interpreted in terms of the properties of the component parts of a material, and the way in which those are assembled. Tensile strength quantifies the force needed to stretch a fabric to the stage where it breaks; in other words, it is the maximum amount of tensile stress that a material can withstand before failure occurs.

Yield strength is defined as the point of stress a material can withstand before it is deformed by 0.2% of the original dimension. A material is distorted elastically prior to reaching the yield point, and returns to its original shape with the removal of stress. Beyond the yield point, the deformation developed remains irreversible.

#### **1.5. Fracture Toughness**

Toughness is the ability of a material to absorb energy and plastically deform without fracturing. One definition of material toughness is the amount of energy per unit volume that a material can absorb before rupturing. It is also defined as a material's resistance to fracture when stressed. Toughness requires a balance of strength and ductility.

Toughness can be determined by integrating the stress-strain curve. It is the energy of mechanical deformation per unit volume prior to fracture.

Another definition is the ability to absorb mechanical energy up to the point of failure. The area under the stress-strain curve is called toughness.

Mathematically, the modulus of resilience can be expressed by the product of the square of the yield stress divided by two times the Young's modulus of elasticity.

Fracture toughness has been calculated by following formula-

$$K_s = 1.5FLa^{0.5}/bw^2[\{1.99-a/w(1-a/w)(2.15-3.93a/w+2.7(a/w)^2)\}/\{(1+2a/w)(1-2a/w)^{1.5}\}]$$

Where F is the fracture load, L is the span of the loading, b is the thickness of specimen, w is the width of specimen and a is the length of the notch.

### **1.6. Flexural strength**

Flexural strength, also known as modulus of rupture, or bend strength, or transverse rupture strength is a material property, defined as the stress in a material just before it yields in a flexure test. The transverse bending test is most frequently employed, in which a specimen having either a circular or rectangular cross-section is bent until fracture or yielding using a three point flexural test technique. The flexural strength represents the highest stress experienced within the material at its moment of yield. It is measured in terms of stress.

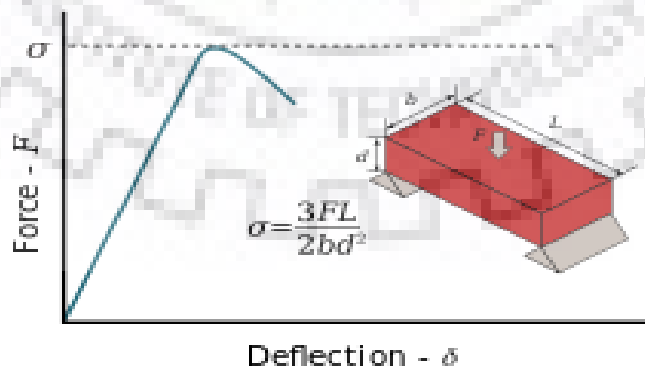


**Fig2 Flexural stress is the Stress at failure**



When an object formed of a single material, like a wooden beam or a steel rod, is bent (Fig. 2), it experiences a range of stresses across its depth (Fig. 3). At the edge of the object on the inside of the bend (concave face) the stress will be at its maximum compressive stress value. At the outside of the bend (convex face) the stress will be at its maximum tensile value. These inner and outer edges of the beam or rod are known as the 'extreme fibers'. Most materials generally fail under tensile stress before they fail under compressive stress, so the maximum tensile stress value that can be sustained before the beam or rod fails is its flexural strength.

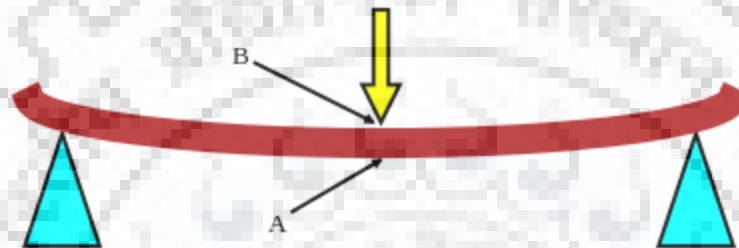


**Fig3 Beam of material under bending. Extreme fibers at B (compression) and (tension)**

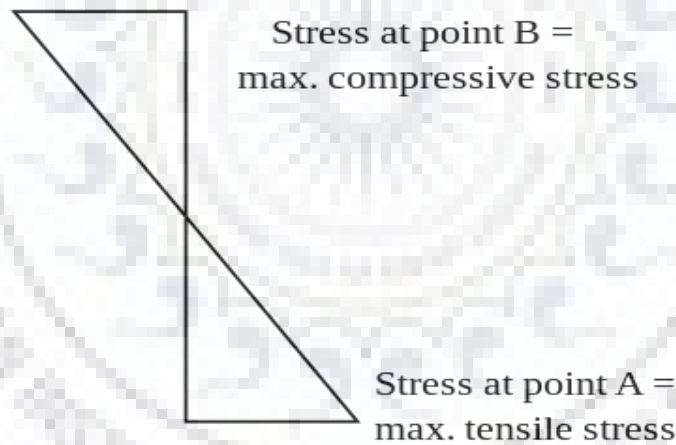


**Fig. 4 - Stress distribution across beam**

### **1.7. Flexural v/s Tensile Strength**

The flexural strength would be the same as the tensile strength if the material were homogeneous. In fact, most materials have small or large defects in them which act to concentrate the stresses locally, effectively causing a localized weakness. When a material is bent only the extreme fibers are at the largest stress so, if those fibers are free from defects, the flexural strength will be controlled by the strength of those intact 'fibers'. However, if the same

material was subjected to only tensile forces then all the fibers in the material are at the same stress and failure will initiate when the weakest fiber reaches its limiting tensile stress. Therefore, it is common for flexural strengths to be higher than tensile strengths for the same material. Conversely, a homogeneous material with defects only on its surfaces (e.g., due to scratches) might have a higher tensile strength than flexural strength.

If we don't take into account defects of any kind, it is clear that the material will fail under a bending force which is smaller than the corresponding tensile force. Both of these forces will induce the same failure stress, whose value depends on the strength of the material.

For a rectangular sample, the resulting stress under an axial force is given by the following formula:

$$\sigma = F/bd$$

This stress is not the true stress, since the cross section of the sample is considered to be invariable (engineering stress).

- $F$  is the axial load (force) at the fracture point
- $b$  is width
- $d$  is the depth or thickness of the material

The resulting stress for a rectangular sample under a load in a three-point bending setup (Fig. 3) is given by the formula below (see "Measuring flexural strength").

The equation of these two stresses (failure) yields:

$$\sigma = 3FL/2bd^2$$

Whereas the strain is given by:

$$e = 6sd/L^2$$

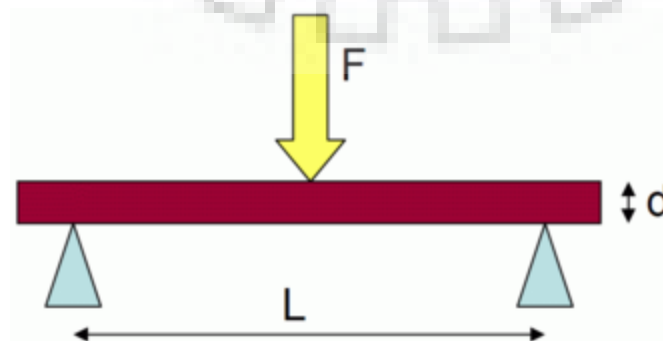


**Fig5 Beam under 3 point bending**

## **1.8. Hardness**

As of the direction of materials science continues towards studying the basis of properties on smaller and smaller scales, different techniques are used to quantify material characteristics and tendencies. Measuring mechanical properties for materials on smaller scales, like thin films, cannot be done using conventional uniaxial tensile testing. As a result, techniques testing material "hardness" by indenting a material with an impression have been developed to determine such properties.

Hardness measurements quantify the resistance of a material to plastic deformation. Indentation hardness tests compose the majority of processes used to determine material hardness, and can be divided into two classes: micro indentation and macro indentation tests. Micro indentation tests typically have forces less than 2 N. Hardness, however, cannot be considered to be a fundamental material property. Instead, it represents an arbitrary quantity used to provide a relative idea of material properties. As such, hardness can only offer a comparative idea of the material's resistance to plastic deformation since different hardness techniques have different scales.

The main sources of error with indentation tests are poor technique, poor calibration of the equipment, and the strain hardening effect of the process. However, it has been experimentally determined through "strainless hardness tests" that the effect is minimal with smaller indentations.

Surface finish of the part and the indenter do not have an effect on the hardness measurement, as long as the indentation is large compared to the surface roughness. This proves to be useful when measuring the hardness of practical surfaces. It also is helpful when leaving a shallow indentation, because a finely etched indenter leaves a much easier to read indentation than a smooth indenter.

The indentation that is left after the indenter and load are removed is known to "recover", or spring back slightly. This effect is properly known as shallowing. For spherical indenters the indentation is known to stay symmetrical and spherical, but with a larger radius. For very hard materials the radius can be three times as large as the indenter's radius. This effect is attributed to the release of elastic stresses. Because of this effect the diameter and depth of

the indentation do contain errors. The error from the change in diameter is known to be only a few percent, with the error for the depth being greater.

Another effect the load has on the indentation is the piling-up or sinking-in of the surrounding material. If the metal is work hardened it has a tendency to pile up and form a "crater". If the metal is annealed it will sink in around the indentation. Both of these effects add to the error of the hardness measurement.

The equation based definition of hardness is the pressure applied over the contact area between the indenter and the material being tested. As a result hardness values are typically reported in units of pressure, although this is only a "true" pressure if the indenter and surface interface is perfectly flat.



## **Aims and Objective**

The present work aims at

- To make Aluminium ZrB<sub>2</sub> composites of 3,6wt% by simple casting method and ultrasonication and observe the micro structure with SEM.
- Perform Tensile, Hardness and 3 Point Bending, Hardness Test and get the values of UTS, Flexural Strength, Fracture Toughness and Hardness for composites and Al 6061 sample. Thus study the mechanical behavior of materials made.
- Draw the Graphs and compare the values.

## **2. Literature Review**

Aluminium is identified as important material in a manufacturing system for exhibiting light weight with high strength in automobile and aerospace applications. Aluminium metal matrix composites (AMMCs) possess improved properties when compared with monolithic alloys for high strength-weight ratio, high wear resistance and low thermal expansion. With this requirement, Al6061 alloy has proved its existence for good workability, good weldability and excellent corrosion resistance. Silicon carbide and aluminium oxides were extensively used as reinforcement during earlier decades of developing AMMCs. Newer trends have been existed in using different reinforcements such as silicon nitride, boron carbide, aluminium oxide, titanium oxide, titanium boride for fabrication of PMMCs. Among various reinforcements tried out till date, ZrB<sub>2</sub> stands as a popular material with strong covalent bonding with very high melting temperature, superior hardness and strength along with excellent thermal conductivity and thermal shock resistance, to exist as a suitable candidate in critical environments associated with aerospace industry . Composites can be fabricated by two casting methods, firstly by adding the powder externally to the melt through ex-situ synthesis (E.g. Liquid ingot casting and Powder metallurgy) and later by synthesizing the particles within the melt through in-situ synthesis (E.g. Reactive hot pressing, Reactive infiltration, exothermic dispersion and direct melt reaction). Poor wettability, reduced bonding and non-uniform distribution have limited the use of ex-situ castings in engineering applications. It has become very essential to eliminate ex-situ synthesis and promote in-situ reactions for meeting the demands of industrial applications. However, the direct melt reaction process requires agitated time at high temperatures to acquire full incorporation through the response of the additional reactants with liquid metal. Literature has been focused on aluminium composites processed through in-situ technique with different reinforcements in the form of fine particles to investigate the nature and morphology of metal matrix composite and their behavior. Dinharan et al. has developed AA6061 alloy reinforced with ZrB<sub>2</sub> produced by an in-situ reaction between K<sub>2</sub>ZrF<sub>6</sub> and KBF<sub>4</sub> salts. Hardness and

strength of composite increases by increasing ZrB<sub>2</sub> content in matrix alloy. Ramesh et al has developed Al6061-TiB<sub>2</sub> composites through in-situ method using Al-Ti and Al-B master alloys. Tensile strength and Ductility increases in composite with higher content of ZrB<sub>2</sub> elements. Moosavian et al. has prepared ZrB<sub>2</sub>/A356 alloy by in-situ technique using Al-15Zr and Al-8B master alloy. Microscopic study, XRD analysis and Tensile test of extruded composite has been investigated before and after T6 heat treatment and compared with matrix alloy. Tensile test reveals that ultimate tensile strength (UTS) and ductility increases compared to matrix alloy with further increase in UTS and decreasing ductility after T6 heat treatment. Songli Zhang et al. [20] has developed Al-ZrB<sub>2</sub> composites with formation of Al<sub>3</sub>Zr through in-situ reaction and investigated microstructure at room temperature. Morphologies of ZrB<sub>2</sub> and Al<sub>3</sub>Zr elements were in regular tetragonal and hexagonal shapes with a size of about 0.30.5μm. Yutao Zhao et al. has fabricated (Al<sub>3</sub>Zr+ZrB<sub>2</sub>)/Al composites from Al-K<sub>2</sub>ZrF<sub>6</sub>-KBF<sub>4</sub> system and investigated the morphology variations of Al<sub>3</sub>Zr crystal in composites due to the effect of molten temperature. Effect of temperature is more sensitive on morphology of Al<sub>3</sub>Zr particles compared to ZrB<sub>2</sub> element.

### **2.1. Mechanical properties of AA6061/TiC AMCs**

In situ formed TiC particles remarkably improve the micro hardness and UTS of AA6061/TiC AMCs. AA6061/5%TiC AMC exhibits 83% higher micro hardness and 21% higher UTS compared to unreinforced AA6061 alloy. The strengthening of AA6061 by in situ formed TiC particles can be expounded as follows. The interaction between TiC particles and dislocations retards the propagation of cracks during tensile loading. The in situ formed TiC particles are defect-free which retain their integrity during tensile loading. The grain refinement caused by the in situ TiC particles increases the area to resist the tensile load and strengthens the composite according to well-known Hall–Patch relationship. The homogeneous distribution of TiC particles invokes Orowan strengthening mechanism. The motion of dislocations is restricted by the homogeneous distribution and causes the dislocations to bow around Fig. 7 Effect of TiC content on micro hardness (a), tensile strength (b) and elongation (c) of AA6061/TiC in situ composites the particles. Thus, Orowan loops are created around TiC particles which impede the progress of dislocations. The clear interface and good interfacial bonding delay the detachment of TiC



particles from the aluminum matrix. Therefore, the micro hardness and UTS of AMC are improved by TiC particles. The net effect by aforementioned factors increases as the content of TiC particles increases, which further raises the values of micro hardness and UTS. The elongation of the AMCs drops against the content of TiC particles as presented. The grain refinement and reduction of ductile matrix content reduces the ductility of the AMCs. The fracture morphology of the matrix alloy AA6061 in reveals large and uniformly distributed voids which point to ductile fracture. The fracture morphologies of the synthesized AA6061/TiC AMCs present smaller size voids compared to that of aluminum, which indicate macroscopically brittle fracture and microscopically ductile fracture. The in situ formed TiC particles refine the grain size of aluminum alloy and diminish the ductility, which cause smaller size voids. The ductile shear band in the fracture morphology is a sign that some amounts of ductility is retained by the AMC. Fractured TiC particles stay intact in a number of places which give confirmation.

## **2.2. Refinement of grains effect on YS and UTS of ultrasonically processed aluminium matrix composite with in-situ Al<sub>3</sub>Ti by salt addition**

In the stress-strain curves of base aluminium alloy and the composites are shown observed that all the composites showed higher YS and UTS as compared to aluminium alloy. The improvements in YS are 12%, 25% and 42%, and in UTS are 35%, 45% and 60% for composite, respectively over the starting alloy. Generally, the properties of matrix and reinforcement material govern the tensile properties of the composite material. The compatibility between reinforcement and matrix plays a significant role in improving the mechanical properties. The improvement in YS and UTS may be attributed to the interaction between dislocations and Al<sub>3</sub>Ti particles when load is applied. These reinforcement particles resist the movement of dislocations and contribute to strengthening. Other contributing factors to increase of YS and UTS of the composites are the grain refinement and generation of dislocation density around the Al<sub>3</sub>Ti particles due to the difference in CTEs between Al matrix and Al<sub>3</sub>Ti particle during solidification. It should also be noted that the clean interface between matrix and reinforcement, and better distribution of reinforcement allow efficient load transfer from matrix to reinforcement which resist the crack initiation at the interface. Ductility (% elongation) of composite is improved significantly over the base alloy by 79%, 114% and 205%, respectively due to the retardation of crack propagation by the in-situ Al<sub>3</sub>Ti particles during deformation. Due to the presence of Al<sub>3</sub>Ti particles, the direction of crack growth is altered, which may cause crack branching, bridging and deviation of crack from its preferred path with respect to the loading



direction. These processes consume more energy which ultimately enhances the work of fracture. Therefore, by increasing the resistance to crack propagation, the ductility of in-situ composite can be improved. Another contribution to increased ductility is by the grain refinement wherein finer and more uniform sized grains exhibit better rheology during deformation delaying failure.

### **2.3. Refinement of grain boundaries effect on hardness of ultrasonically processed aluminium matrix composite with in-situ Al<sub>3</sub>Ti by salt addition**

Brinell hardness number of the base aluminium alloy and the composites with 2.7, 5.4 and 8.1wt % of in-situ Al<sub>3</sub>Ti. It is clearly observed that the developed composites possess improved hardness over the starting alloy by 50, 72 and 103%, respectively. It is experimentally proven fact that the hardness of the matrix material is increased when the hard particles are reinforced into the soft ductile matrix. The incorporation of Al<sub>3</sub>Ti particle in the aluminium matrix improves the hardness of the composite and improves its ability to resist deformation. Furthermore, the hardness of the composites improves as the amount of Al<sub>3</sub>Ti is increased. The refinement of matrix phase also contributes to strengthening of the composites because the grain boundaries effectively resist the movement of dislocations during deformation. The generation of dislocation density around Al<sub>3</sub>Ti particles due to difference in CTEs between Al matrix and Al<sub>3</sub>Ti also improves the hardness of the composites. Clean interface and better bonding between matrix and reinforcement increase load bearing capacity of the composite which leads to the improved hardness.

### **2.4. Fracture toughness behavior of in-situ Al-Ti composites produced via mechanical alloying and hot extrusion**

Al-20Ti-4hrV composite sample has very high hardness, modulus and flexural strength compared to the other composites. This result is the consequence of both ultrafine grain size of the matrix and the nanometric particles distributed homogeneously in the Al matrix. As mentioned in our previous paper, the Hall-Petch and Orowan strengthening mechanisms have been distinguished as the main mechanisms of attaining superior properties in this composite. Moreover, the hardness and elastic modulus of other two composites are higher than those of the CGAl sample. However, this trend was not observed in flexural strength due to the presence of

structural defects. Actually, the flattened particles prevent the formation of strong bonding between aluminum and titanium in this composite. Thus, the full consolidation is not achieved and consequently, the density decreases. Besides, the flexural strength of Al-10Ti-60hrP composite reduces in comparison with CGAl..

### **2.5. Effects of ultrasonic vibration treatment on particles distribution of TiB<sub>2</sub> particles reinforced aluminum composites**

The UV treatment effectively improves the particles distribution of TiB<sub>2</sub>p/Al-4.5Cu composites. First of all, the yield strength and UTS of the untreated composite are improved from 64 MPa and 163–74 MPa and 205 MPa compared with the base metal, respectively. These improvements are the result of the combination strengthen of load-bearing strengthening, Orowan strengthening, grain boundary strengthening, CTE (Coefficient of Thermal Expansion) mismatch strengthening and grain refinement. When TiB<sub>2</sub> particles are successfully in-situ formed in the melt and well bonded with the matrix, they can directly shear the load and strengthen the composite according to load-bearing strengthening mechanism. The submicron dispersed TiB<sub>2</sub> particles with high elastic modulus can hinder the dislocation movement and the dislocation line is formed looped around them according to Orowan strengthening mechanism. The interaction of dislocation loops of adjacent TiB<sub>2</sub> particles can obstructed the subsequent dislocation movement and thus strengthen the composite. For the TiB<sub>2</sub> particles gathered at the grain boundary regions, they may not be the suitable reinforcements to form dislocation loops for Orowan strengthening due to the short distance of adjacent particles and some of them are too large. But the particles with high elastic modulus and high hardness can still hinder the dislocation movement at grain boundary, thus the dislocations are stacked at grain boundary regions and strengthen the composite. The TiB<sub>2</sub> particles and aluminum matrix have different CTE and the CTE mismatch generates the residual plastic strain between them after solidification. Then the residual plastic strain generates dislocations to accommodate CTE mismatch at the interface of TiB<sub>2</sub> particles and aluminum matrix and strengthen the composite. The finer grains bring better mechanical properties and the Hall-Petch relationship explains the relationship between the decreasing of grain size and the increasing of yield strength. Therefore the yield strength and UTS of the untreated composite are improved with presence of TiB<sub>2</sub> particles and effectively refined grains. When the composite is treated by UV for 30 s, large aggregates are eliminated which brings

many dispersed particles in the melt. Then there are more particles distributed at grain boundary or as dispersed particles in the matrix after solidification. And the grains of the composite are further refined. So the Orowan strengthening is enhanced with more suitable dispersed particles and the CTE mismatch strengthening is enhanced with enlarged interface of particles and matrix. Therefore, the yield strength of the composite is improved from 74 MPa to 106 MPa. The elimination of large aggregates and refinement of grains also brings more uniformly distributed TiB<sub>2</sub> particles in the enlarged grain boundary regions, the grain boundary strengthening is also enhanced. Therefore the UTS of the composite is increased from 205 MPa to 215 MPa. This improvement of UTS is not very effective and may due to the UV treatment may agitates the oxidation and brings more oxide inclusions into the melt. Cast defects are also affect. When the UV treatment time is extended to 60 s and 120 s, the small aggregates are gradually eliminated and the grains of the composite are further refined. So with the uniform distribution of particles, the strengthening, CTE mismatch strengthening and grain boundary strengthening are further enhanced. Therefore the yield strength and UTS of the composites are all slightly improved with the extension of UV treatment time. The elongation of TiB<sub>2</sub>p/Al-4.5Cu composites either treated by UV or untreated is lower than the base metal. That is due to the particles which gather at the grain boundaries during the solidification may obstruct the deformation of the grains. Through the UV treatment, the large aggregates are eliminated and the particles distribution become more uniform in the melt. But oxide inclusions are increased and show more damage on the ductility. So the elongation of the composites treated by UV is lower than the untreated composite. Among the composites treated by UV, small aggregates are gradually eliminated and the grains of the composites are further refined with the extension of UV treatment time. The distribution of the particles are uniform. Thus the elongation of the composites is slightly increased with the extension of UV treatment time.

## **2.6. Microstructural Study of AA6061/ZrB<sub>2</sub>AMCs by Optical Microscope**

Fig6 records the optical photomicrographs of the prepared AA6061/ZrB<sub>2</sub>AMCs. Fig6a represents the cast aluminum matrix 6061. The micrograph is characterized by a dendritic structure which is commonly found in cast alloys. The composite micrographs do not record Fig6 (b-e) dendritic structure. The formation of ZrB<sub>2</sub> particles drives out dendritic structure from the composite. A clear grain structures evolves due to the reinforcement of ZrB<sub>2</sub> particles. It suggests that in situ synthesized ZrB<sub>2</sub> particles are capable of refining the microstructure. The optical micrographs reveal two kinds of distribution of ZrB<sub>2</sub> particles. Most of the ZrB<sub>2</sub> particles are driven to grain boundaries regions at a weight fraction of 3. Large clusters are formed at 6wt% and those clusters are trapped within the grain boundaries. The tendency to form clusters increase with higher content of reinforcement particles. Such formation of clusters within grain boundaries in AMCs by in situ method. The factors which cause clusters to be moved inside grain boundaries are slow cooling velocity and lower thermal conductivity ratio between the particle and the molten aluminum. The two kinds of distributions are known as inter granular and intra granular distribution respectively. The former is preferred over the latter for better mechanical properties. Pushing or engulfing of particles is dictated by the velocity of the solidification front. Lower velocity compared to the threshold value results in pushing of particles and vice versa. The high intensity ultrasonic vibrations are applied into the melt to break the agglomerated ZrB<sub>2</sub> particles and achieve better distribution throughout the matrix as observed in Fig6(c and e). During ultrasonic treatment, ultrasonic field injected into the molten metal produce nonlinear effects such as acoustic streaming and cavitation. In cavitation, small cavities are formed throughout the molten metal when the acoustic wave produces tensile stress during the rarefaction phase. The size of these cavities increases due to inertia, until a stage comes when they collapse because of compressive stress during the compressive phase of the cycle.



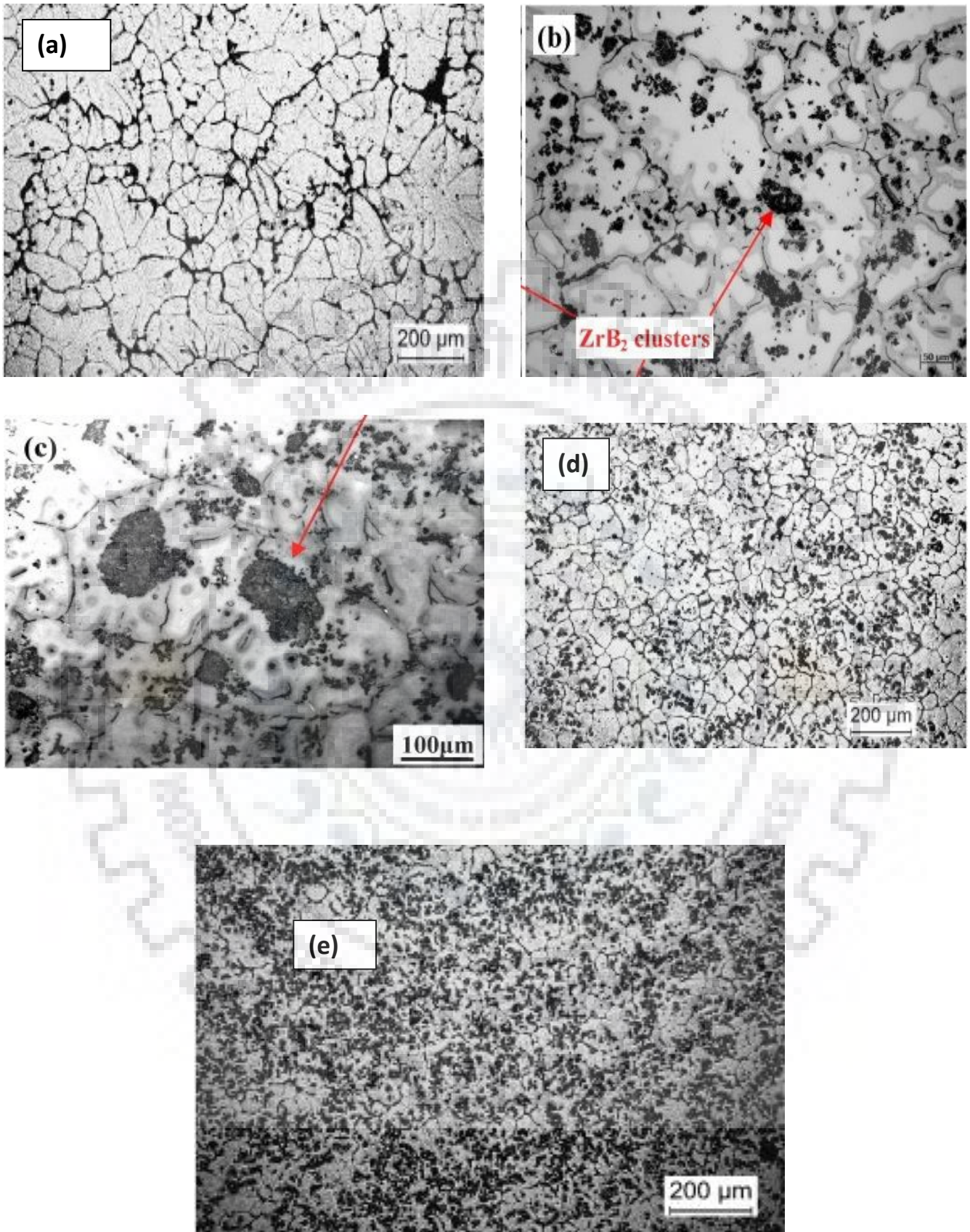


**Fig. 6. Optical micrographs of AA2024/ZrB<sub>2</sub> in situ composites containing ZrB<sub>2</sub>: (a) 0 wt%, (b) 3wt%, (d) 6 wt % ,(c) 3 wt% with ultrasonication, and (e) 6 wt% with ultrasonication**

### **3. Plan of work**

Aluminium alloy AA6061 was used as a matrix material. The chemical analysis of Al6061 alloy was done by XRF (Rigaku supermini 200) and presented in Table 1.

In order to make composites of 3, 6 wt% ZrB<sub>2</sub> by simple casting the ingot was taken inside a graphite crucible and heated up to 850°C in a resistance heating furnace. After holding the melt at 850°C for 30min, the measured quantity of inorganic salts K<sub>2</sub>ZrF<sub>6</sub> and KBF<sub>4</sub> were incorporated into the aluminium melt to develop composites with different weight percent (3,6wt %) of ZrB<sub>2</sub> particles as shown in. After addition, the melt was stirred manually for 2min by using a graphite rod for proper mixing of the powders into the molten metal. After the execution of the process, the composite mixture was poured into cast iron molds that are kept ready preheated. The experimental setup is shown in Fig. 6.

After it another samples were made with ultrasonication. For that after proper mixing of the salt, ultrasonication was carried out at 850°C for 5min. The schematic diagram of ultrasonically assisted casting is illustrated in Fig. 3. A 1.5kW high power ultrasonic system (Model VCX 1500, Sonics and Materials, USA), which could produce 20 kHz frequency with air cooled converter, made from piezoelectric crystals, was used for generating ultrasonic vibration in the molten melt. The intensity of this unit could be adjusted from 0to5.4kWcm<sup>-2</sup>.

**Table 1. Chemical composition of Al6061 alloy.**

Elements	Si	Fe	Cu	Mn	Mg	Cr	Zn	Ti	Al
Wt%	0.70	0.18	0.29	0.33	0.88	0.006	0.003	0.02	97.591

250 g of aluminum 6061 heated to 850 °C in a graphite crucible.

After holding the melt at 850°C for 30min, the measured quantity of inorganic salts K<sub>2</sub>ZrF<sub>6</sub> and KBF<sub>4</sub> were incorporated into the aluminium melt

Ultrasonication was carried out at 850°C for 5min

- SEM
- XRD
- TENSILE TEST
- 3 POINT BENDING TEST
- Brinell Hardness Test

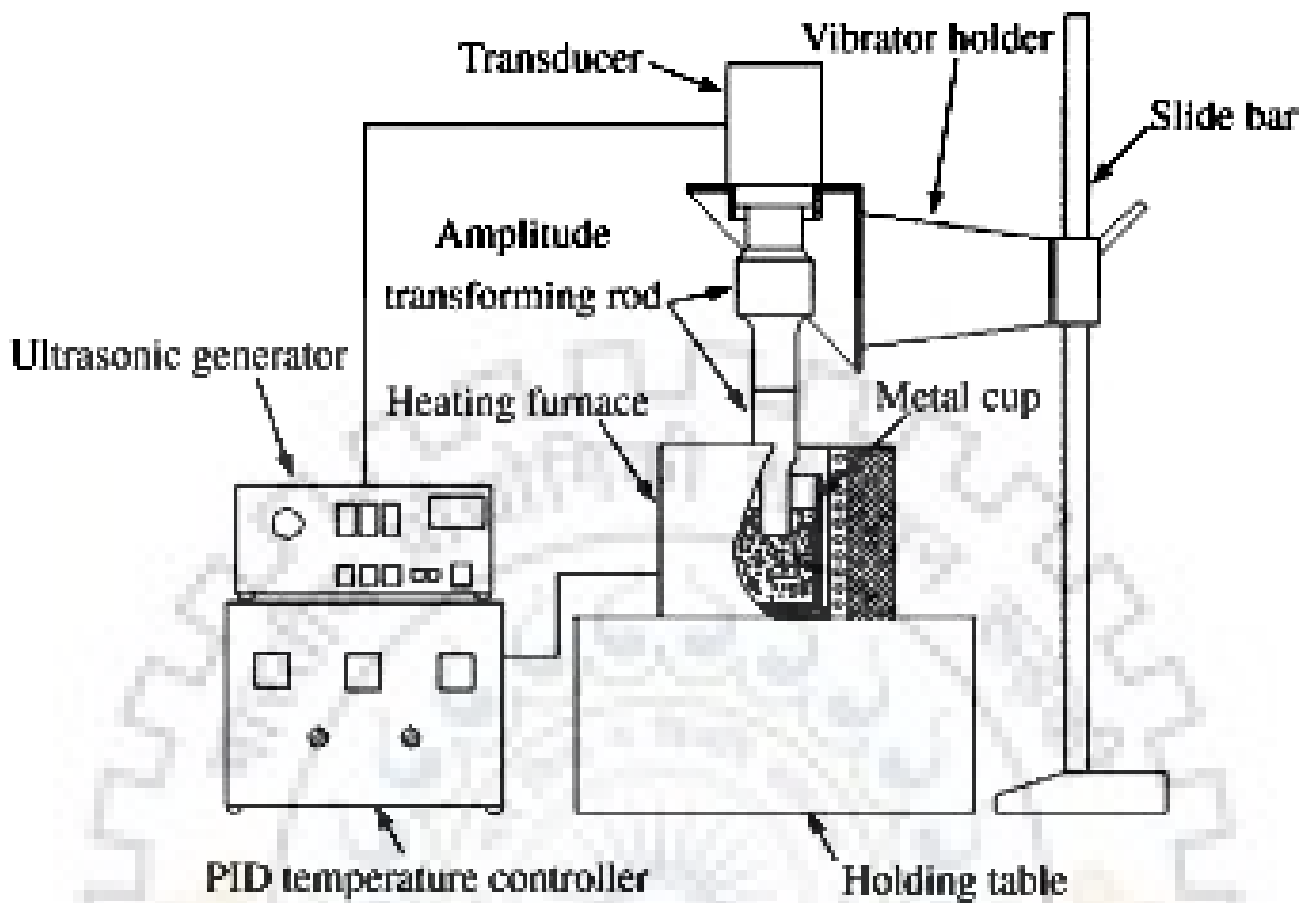


**Fig7 Experimental setup with ultrasonic transducer**

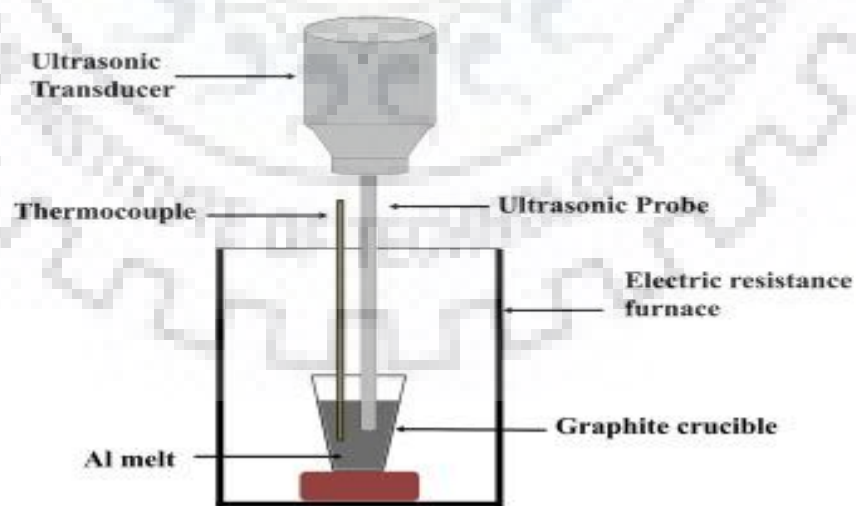


**Fig8 Schematic diagram of ultrasonic assisted casting**



## **4. Experimental Procedure**

After ultrasonication, the melt was poured and allowed to solidify in a mild steel mold of dimension  $40 \times 40 \times 120 \text{ mm}^3$  which was coated with Zirconia to avoid contamination from the mold. The mold was preheated to  $400 \text{ }^\circ\text{C}$  to ease the flow and reduce thermal damage to the casting. Metallographic samples were cut from the cast ingot and polished with 320, 800, 1200, 1500 and 2000 grit emery papers followed by cloth polishing with MgO abrasive. These polished samples were etched with Keller's reagent to obtain the microstructure. Optical microscope (Leica, DMI 5000 M) and scanning electron microscope (Carl Zeiss, EVO 18) in secondary electron imaging mode were used for imaging. The mean linear intercept method was used to calculate average grain size. The XRD analysis was conducted using Rigaku smart lab, X-ray diffractometer employing Cu  $K\alpha$  radiation. Tensile test was performed at room temperature on a H25 K-S Tinius Olsen tensile testing machine with constant crosshead speed of  $0.1 \text{ mm/min}$ . The dimensions of tensile specimen were 4 mm diameter and 20 mm gauge length according to the ASTM E&M standard and tensile testing was carried out according to ASTM B557 with a strain rate of  $10^{-3}/\text{s}$ . The average value of three tensile tests is reported along with standard deviation. Hardness test was performed on HPO-250 Heckert Brinell hardness tester with 1 kgf load. An average of at least five hardness readings was taken and reported along with standard deviation.

**Table 2 Samples and their Compositions.**

<b>Samples</b>	<b>Description</b>	<b>Al 6061</b>	<b>K2ZrF6</b>	<b>KBF<sub>4</sub></b>
<b>C 0</b>	Al 6061 Base Alloy	250	0	0
<b>C 3</b>	Al 6061 3wt% ZrB <sub>2</sub> by simple casting	250	18.8482	23.5609
<b>C 3U</b>	Al 6061 3wt% ZrB <sub>2</sub> with UV casting.	250	37.6964	47.1204
<b>C 6</b>	Al 6061 6wt% ZrB <sub>2</sub> by simple casting	250	56.5445	70.6806
<b>C 6U</b>	Al 6061 3wt% ZrB <sub>2</sub> with UV casting.	250	75.3769	94.2409

## 5. Results and discussions

### 5.1 XRD Analysis

Figure 8 illustrates the XRD patterns obtained for the produced composites and these confirm the occurrence of ZrB<sub>2</sub> reinforcement within the base matrix. The diffraction peaks of in situ formed ZrB<sub>2</sub> particles as well as of the monolithic matrix aluminum alloy were clearly noticeable. They increase with the increase in ZrB<sub>2</sub> contents while the peaks of AA6061 decrease. It is also interesting to note that the peaks of aluminum in the composite are gradually and marginally shifted to lower 2θ as compared to that of AA6061 alloy. The XRD pattern also indicates the formation of ZrB<sub>2</sub> particles without the presence of any other intermetallic compounds

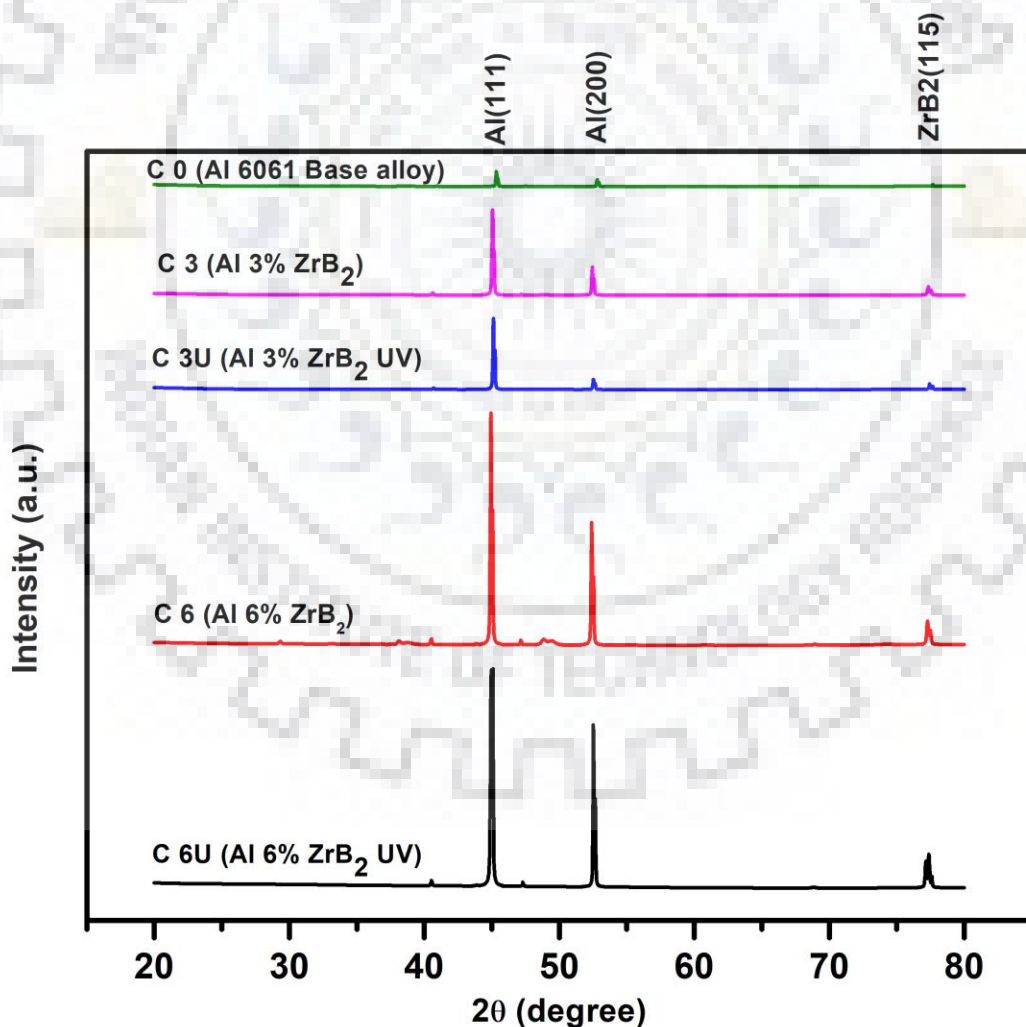
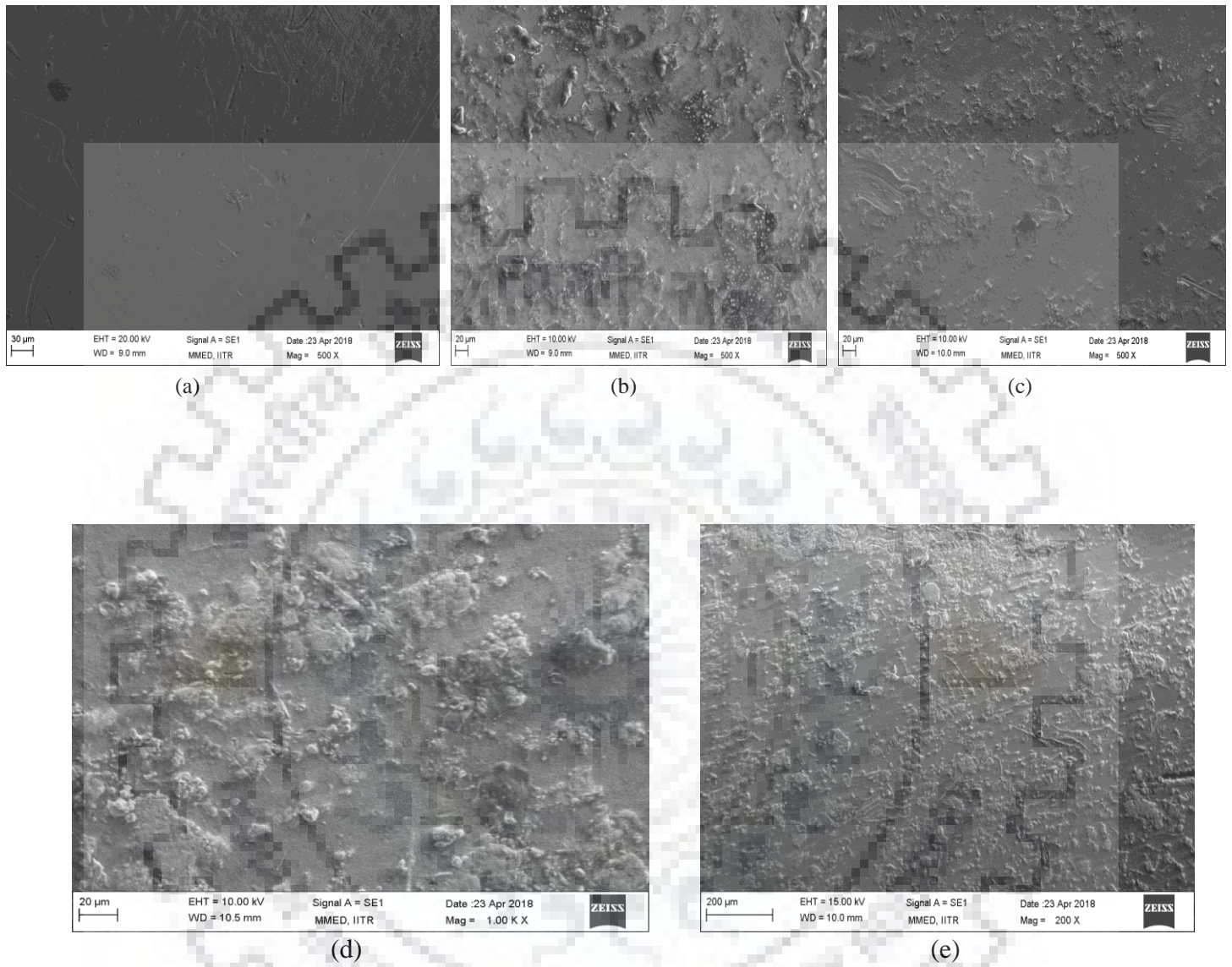


Fig9 XRD patterns of the fabricated composites and base Al alloy.

## **5.2. Microstructural Study**

Fig10 represents the SEM micrographs of the prepared AA6061/ZrB<sub>2</sub>AMCs. SEM micrographs confirm the observation of optical microscopy. There is a continuous distribution of ZrB<sub>2</sub> particles in the aluminum matrix. There are no vast areas unreinforced with particles. This kind of distribution is desirable which helps to improve the properties. The particles should be suspended in the melt for longer duration with minimum displacement to obtain good distribution. The distribution within the molten aluminum during casting is influenced by several factors. One major factor is density gradient between the molten aluminum and ceramic particles. In situ method produces sub-micron and nano level particles. Subsequently, it will take more time for the ZrB<sub>2</sub> particle to sink to the bottom of the crucible. The action of molten aluminum wetting the surface of newly formed ZrB<sub>2</sub> particles restricts the free movement. Therefore, ZrB<sub>2</sub> particles are continuously distributed over the entire aluminum matrix. The increase in weight percentage of ZrB<sub>2</sub> particles increases the viscosity of the melt. The ultrasonication reduces the particle size further and causes the better distribution.



**Fig 10 SEM micrographs of AA6061/ZrB<sub>2</sub> in situ composites containing ZrB<sub>2</sub>: (a) 3 wt%, (b) 3 wt% with ultrasonication(c) 6 wt% and (d) 6 wt% with ultrasonication..**

### **5.3. Tensile strength**

The stress-strain curves of base aluminium alloy and the composites are shown in fig11. Their average UTS and % elongation values are listed in table 3. It is observed that all the composites showed higher YS and UTS as compared to aluminium alloy. The improvements in UTS are 7.42%, 17.18%, 32.81%, 40.625% for C3, C3U, C6 and C6U composite, respectively over the starting alloy. Generally, the properties of matrix and reinforcement material govern the tensile properties of the composite material. The compatibility between reinforcement and matrix plays a significant role in improving the mechanical properties. The improvement in YS and UTS may be attributed to the interaction between dislocations and  $ZrB_2$  particles when load is applied. These reinforcement particles resist the movement of dislocations and contribute to strengthening. Other contributing factors to increase of YS and UTS of the composites are the grain refinement and generation of dislocation density around the  $ZrB_2$  particles due to the difference in CTEs between Al matrix and  $ZrB_2$  particle during solidification. It should also be noted that the clean interface between matrix and reinforcement, and better distribution of reinforcement allow efficient load transfer from matrix to reinforcement which resist the crack initiation at the interface.

Ductility (% elongation) of C3, C3U, C6 and C6U composite is improved significantly over the base alloy by 15%, 20%, 37%, and 50%, respectively due to the retardation of crack propagation by the in-situ  $ZrB_2$  particles during deformation. Due to the presence of  $ZrB_2$  particles, the direction of crack growth is altered, which may cause crack branching, bridging and deviation of crack from its preferred path with respect to the loading direction. These processes consume more energy which ultimately enhances the work of fracture. Therefore, by increasing the resistance to crack propagation, the ductility of in-situ composite can be improved. Another contribution to increased ductility is by the grain refinement wherein finer and more uniform sized grains exhibit better rheology during deformation delaying failure.



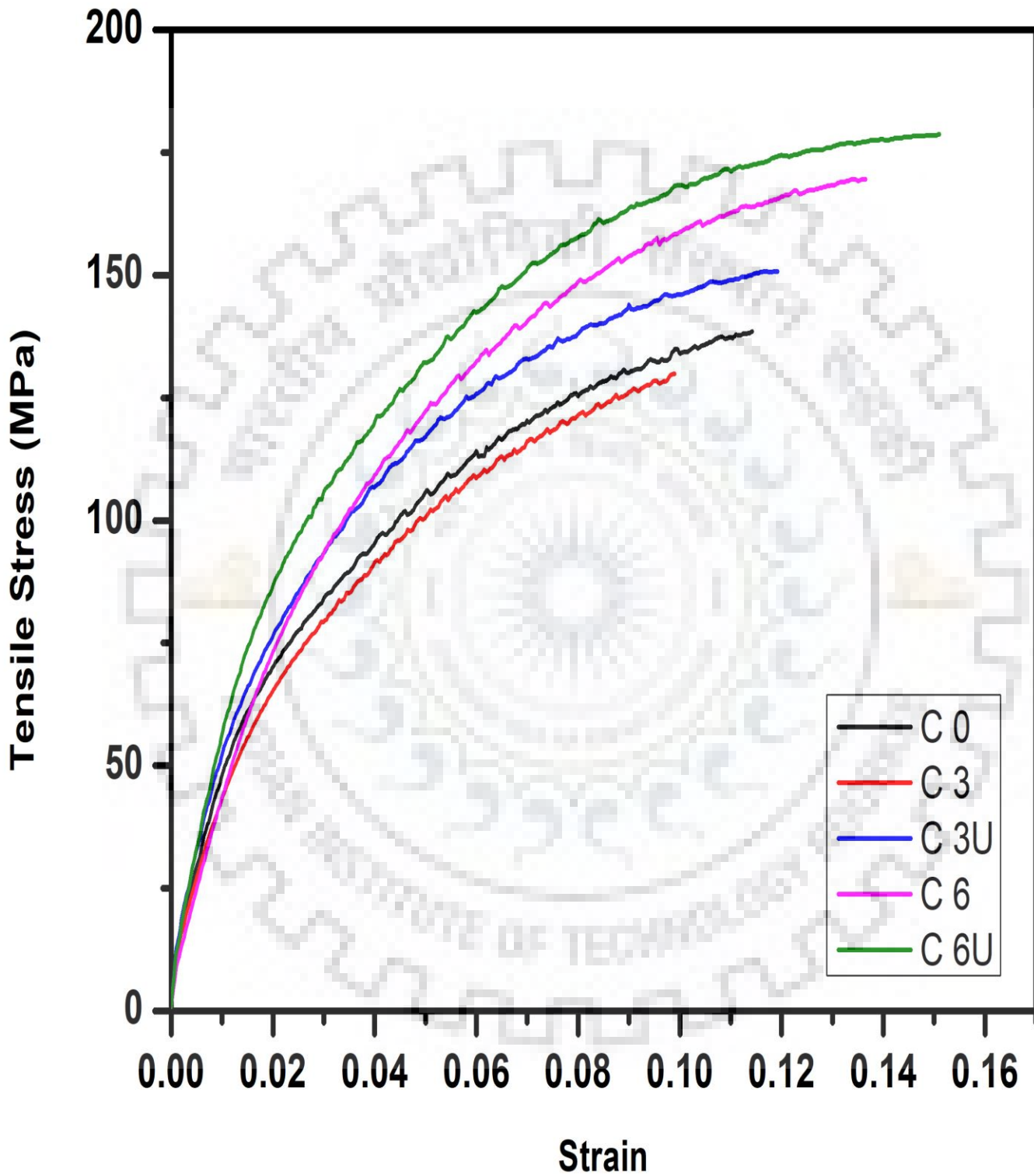


Fig. 11. Engineering stress-engineering strain curves of base Al alloy and composites.

**Table 3. UTSs, Elongations and %Increases**

Composites	UTS(MPa)	%Increase in UTS	Elongation(mm)	% Increase in Elongation
C0	128		0.1	
C3	137.5	7.42	0.115	15
C3U	150	17.18	0.12	20
C6	170	32.81	0.137	37
C6U	180	40.625	0.15	50

#### **5.4. Hardness**

Fig12 shows the Brinell hardness number of the base aluminium alloy and the composites with 3wt%, 3wt% by ultrasonication, 6%, 6wt% by ultrasonication of in-situ ZrB<sub>2</sub>. It is clearly observed that the developed composites possess improved hardness over the starting alloy by 50, 72 and 103%, respectively. It is experimentally proven fact that the hardness of the matrix material is increased when the hard particles are reinforced into the soft ductile matrix. The incorporation of ZrB<sub>2</sub> particle in the aluminium matrix improves the hardness of the composite and improves its ability to resist deformation. Furthermore, the hardness of the composites improves as the amount of ZrB<sub>2</sub> is increased. The refinement of matrix phase also contributes to strengthening of the composites because the grain boundaries effectively resist the movement of dislocations during deformation. The generation of dislocation density around ZrB<sub>2</sub> particles due to difference in CTEs between Al matrix and ZrB<sub>2</sub> also improves the hardness of the composites. Clean interface and better bonding between matrix and reinforcement increase load bearing capacities of the composite which leads to the improved hardness.

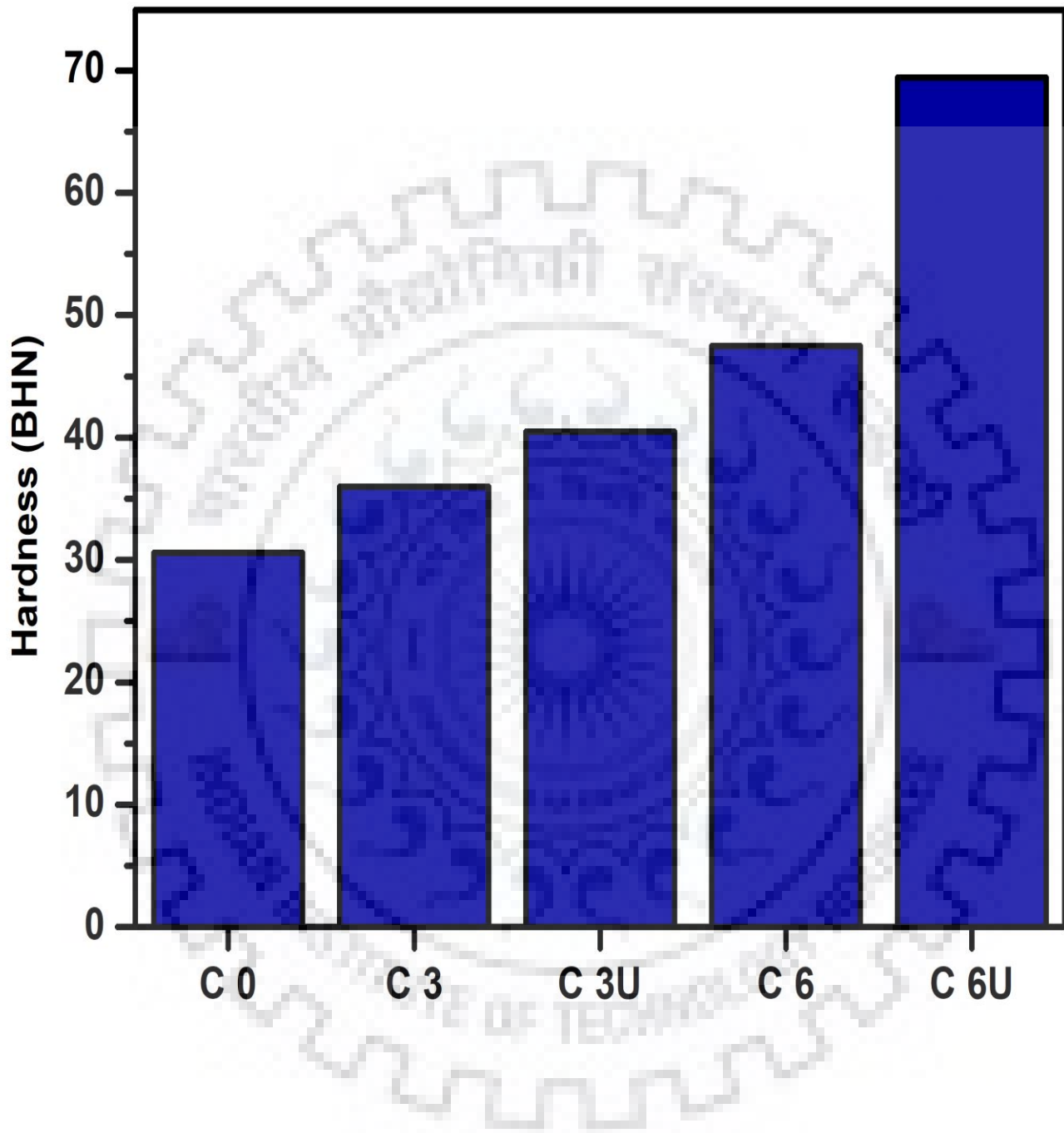


**Fig. 12. Variation in hardness of base Al alloy and the developed composites.**



## **5.5 Flexural Strength**

The measured value of flexural strength for the base alloy Al 6061 can be compared with those of composites C3, C3U, C6 and C6U as shown in fig 13. The corresponding values of flexural strain and strengths are given in table 4. The incorporation of ZrB<sub>2</sub> particles increases the flexural strength of the in-situ composite compared that of Al 6061. The studied in-situ composite suffer from a lack of intrinsic toughening mechanisms due to absence of mobile dislocations which can form a plastic zone ahead of crack tip. Hence, the improvement of the flexural strength can be related to extrinsic toughening mechanisms namely to crack deviation, zone shielding by micro crack toughening and bridging by ZrB<sub>2</sub> particles. However, the effectiveness of these extrinsic toughening mechanisms depends strongly on the applied processing techniques, volume fraction and size of the ZrB<sub>2</sub> particles. The incorporation of the ZrB<sub>2</sub> particles into Al 6061 matrix has improved flexural strength of the in-situ composites

**Table 4 Flexural Strength and Strain values**

<b>Composites</b>	<b>Flexural Strength(Mpa)</b>	<b>Flexural Strain</b>	<b>Extension at Flexural Point(mm)</b>
<b>C 0</b>	210	0.025	0.019
<b>C 3</b>	355	0.035	0.025
<b>C 3U</b>	375	0.04	0.030
<b>C 6</b>	395	0.05	0.0375
<b>C 6U</b>	415	0.07	0.05

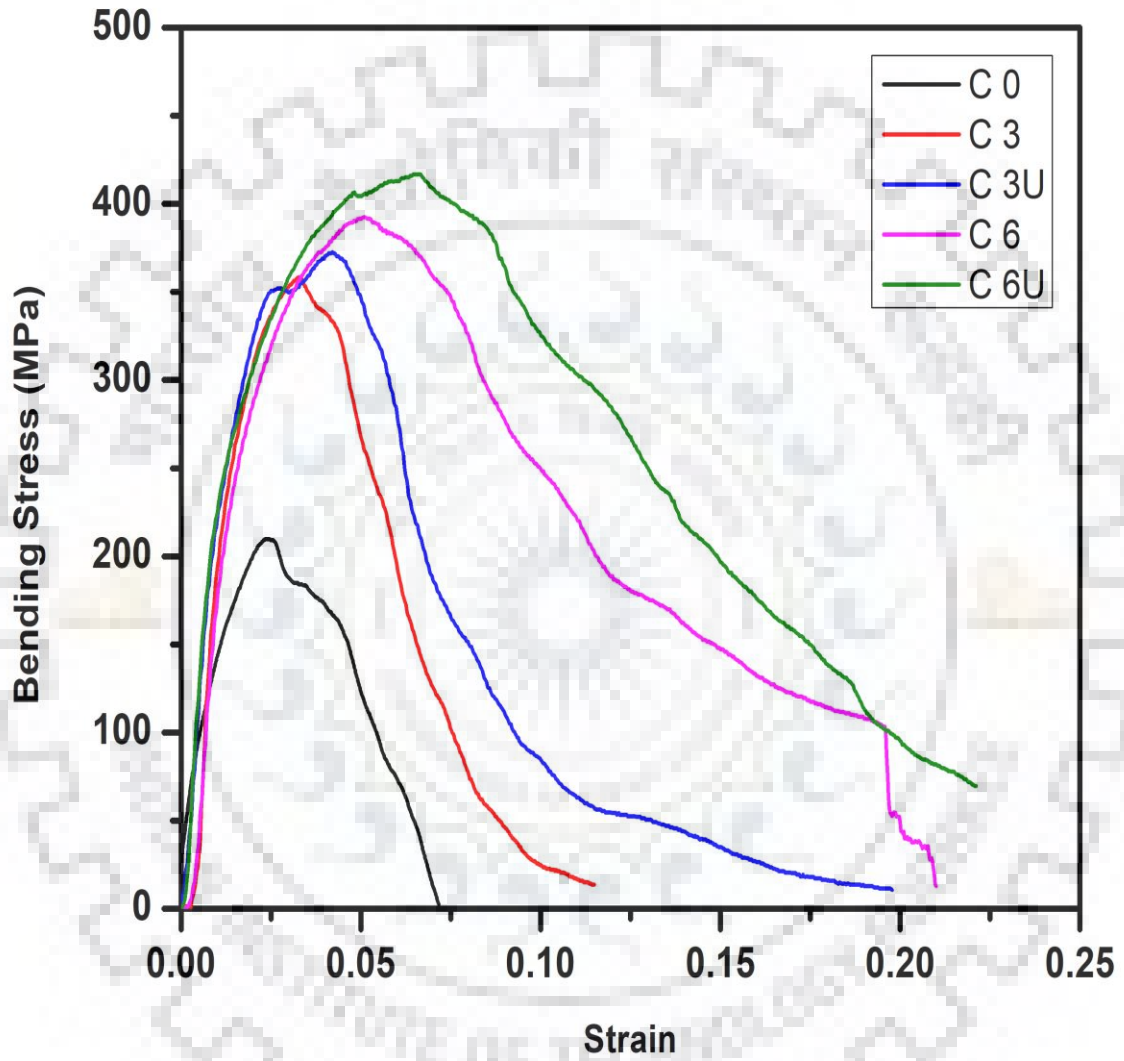


Fig 13 Flexural Stress-Strain curve of base Al alloy and the developed composites.

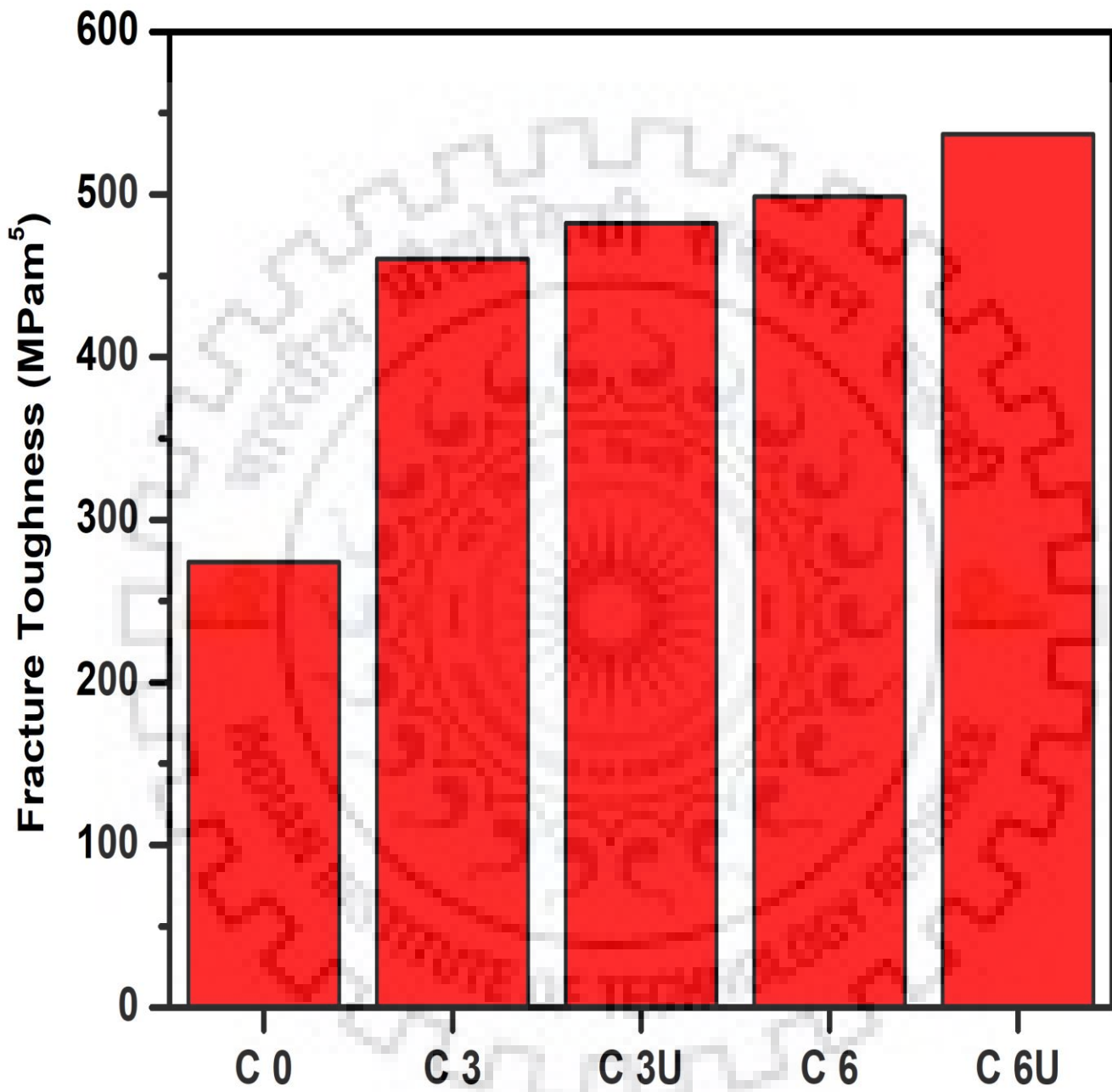
## **5.6 Fracture Toughness**

The incorporation of ZrB<sub>2</sub> particles increases the fracture toughness of the in-situ composite compared those of base alloy Al 6061. The studied in-situ composite suffer from a lack of intrinsic toughening mechanisms due to absence of mobile dislocations which can form a plastic zone ahead of crack tip. Hence, the improvement of the fracture toughness can be related to extrinsic toughening mechanisms namely to crack deviation, zone shielding by micro crack toughening and bridging by coarse lathe-shaped carbide particles. However, the effectiveness of these extrinsic toughening mechanisms depends strongly on the applied processing techniques, volume fraction and size of the ZrB<sub>2</sub> particles. The incorporation of the ZrB<sub>2</sub> particles into Al 6061 matrix has improved fracture toughness of the in-situ composites.

Table 5 lists the Fracture Toughness values obtained for base alloy and composites and % increase in Fracture Toughness values. Fig 14 shows the graph of variation in toughness values.

**Table 5 Values of Fracture Toughness**

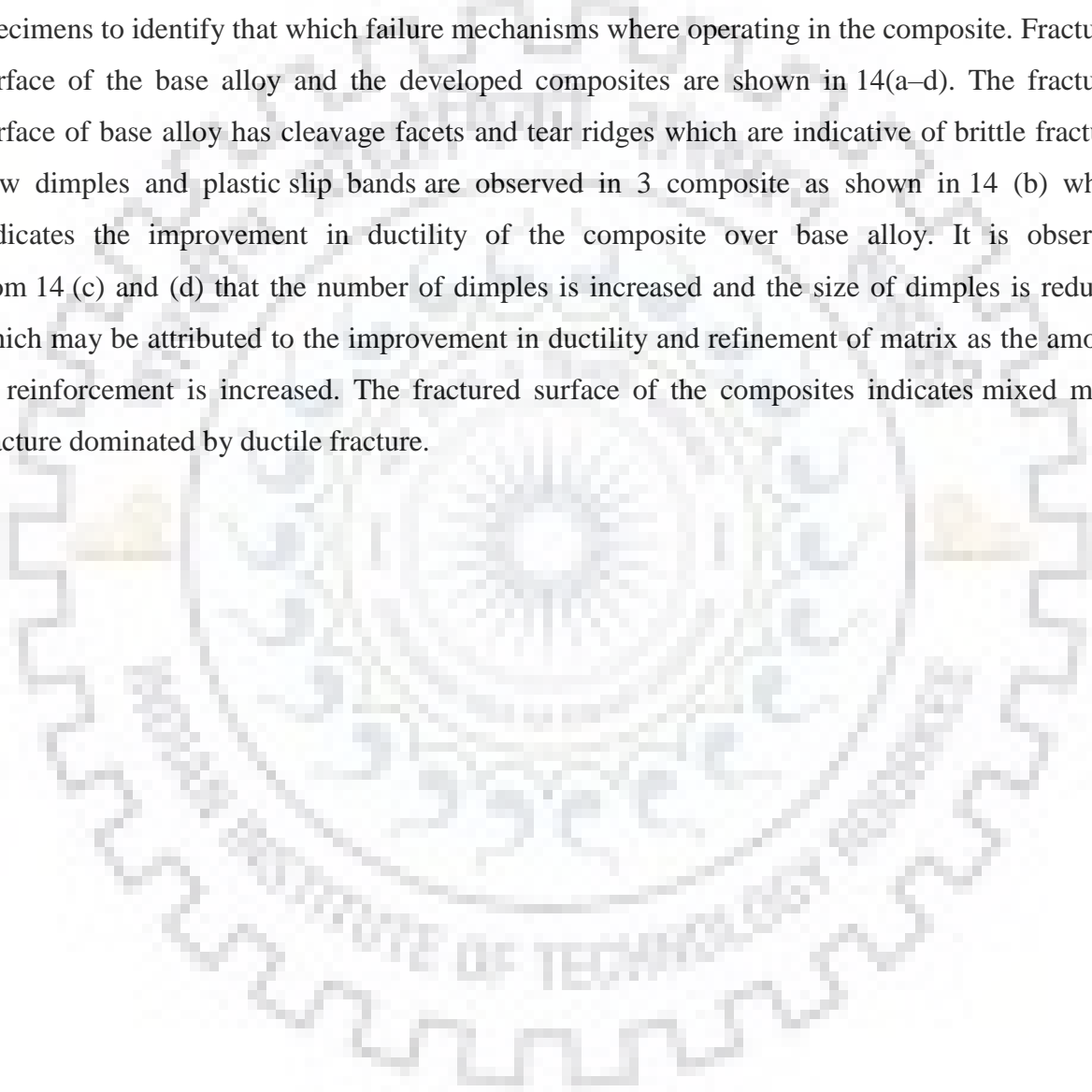
<b>Composites</b>	<b>Load at Flexural Point(N)</b>	<b>Fracture Toughness(MPam<sup>0.5</sup>)</b>	<b>% Increase</b>
<b>C 0</b>	250	274.0325	
<b>C 3</b>	420	460.3746	68.8899
<b>C3U</b>	440	482.2972	75.912
<b>C 6</b>	455	498.7391	81.7518
<b>C 6U</b>	490	537.1037	95.9845



**Fig 14** Variation in Fracture Toughness of base Al alloy and the developed composites.

## **5.6 Fractography**

The fracture surface analysis is very helpful to identify the contribution made by different mechanism to failure process and to identify the dominant failure mechanism. Therefore, fractographical examination which has been successfully used to understand the failure mechanism of monolithic metals, was conducted on the fractured surface of the tensile specimens to identify that which failure mechanisms were operating in the composite. Fractured surface of the base alloy and the developed composites are shown in 14(a-d). The fractured surface of base alloy has cleavage facets and tear ridges which are indicative of brittle fracture. Few dimples and plastic slip bands are observed in 3 composite as shown in 14 (b) which indicates the improvement in ductility of the composite over base alloy. It is observed from 14 (c) and (d) that the number of dimples is increased and the size of dimples is reduced which may be attributed to the improvement in ductility and refinement of matrix as the amount of reinforcement is increased. The fractured surface of the composites indicates mixed mode fracture dominated by ductile fracture.





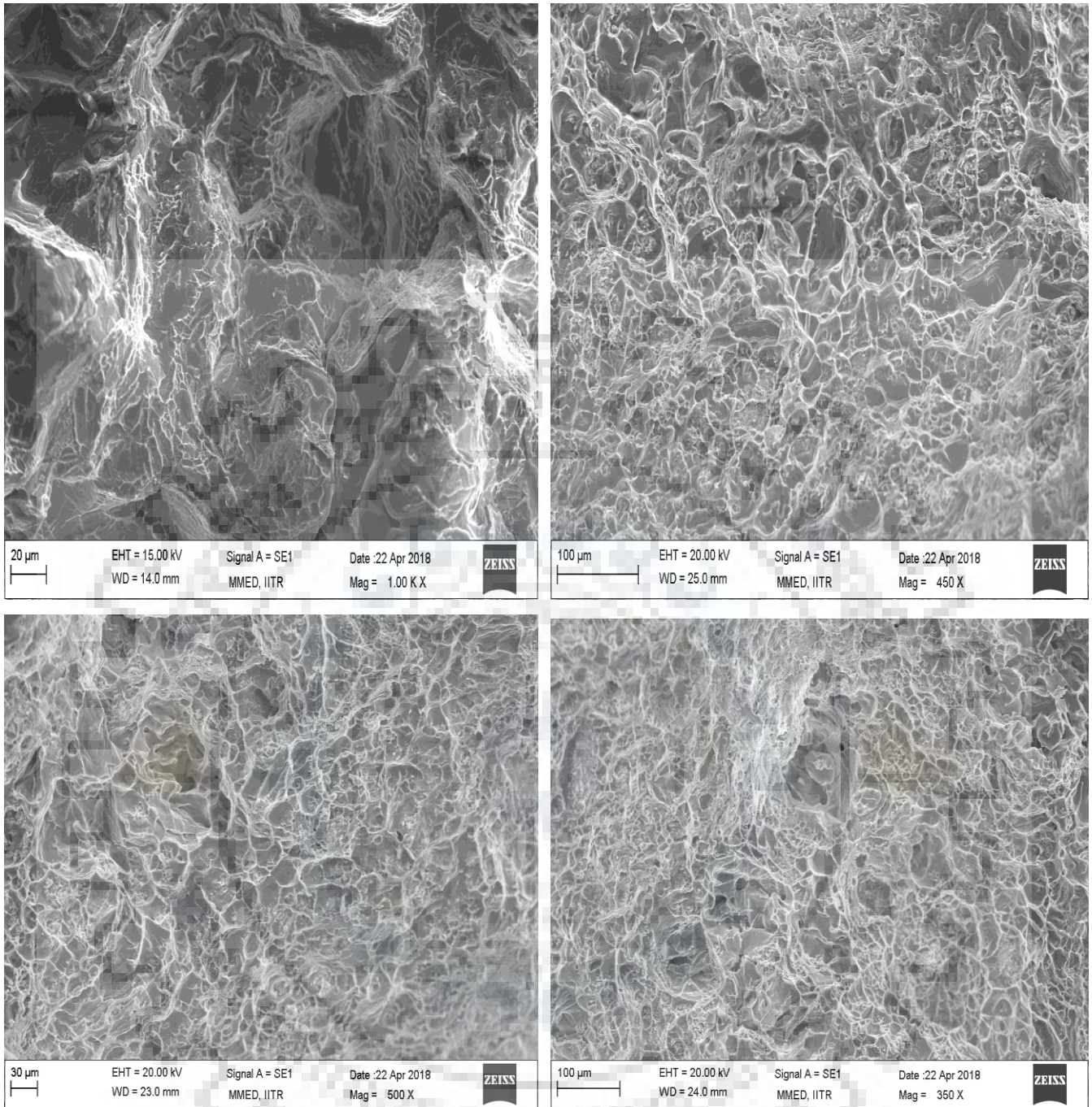
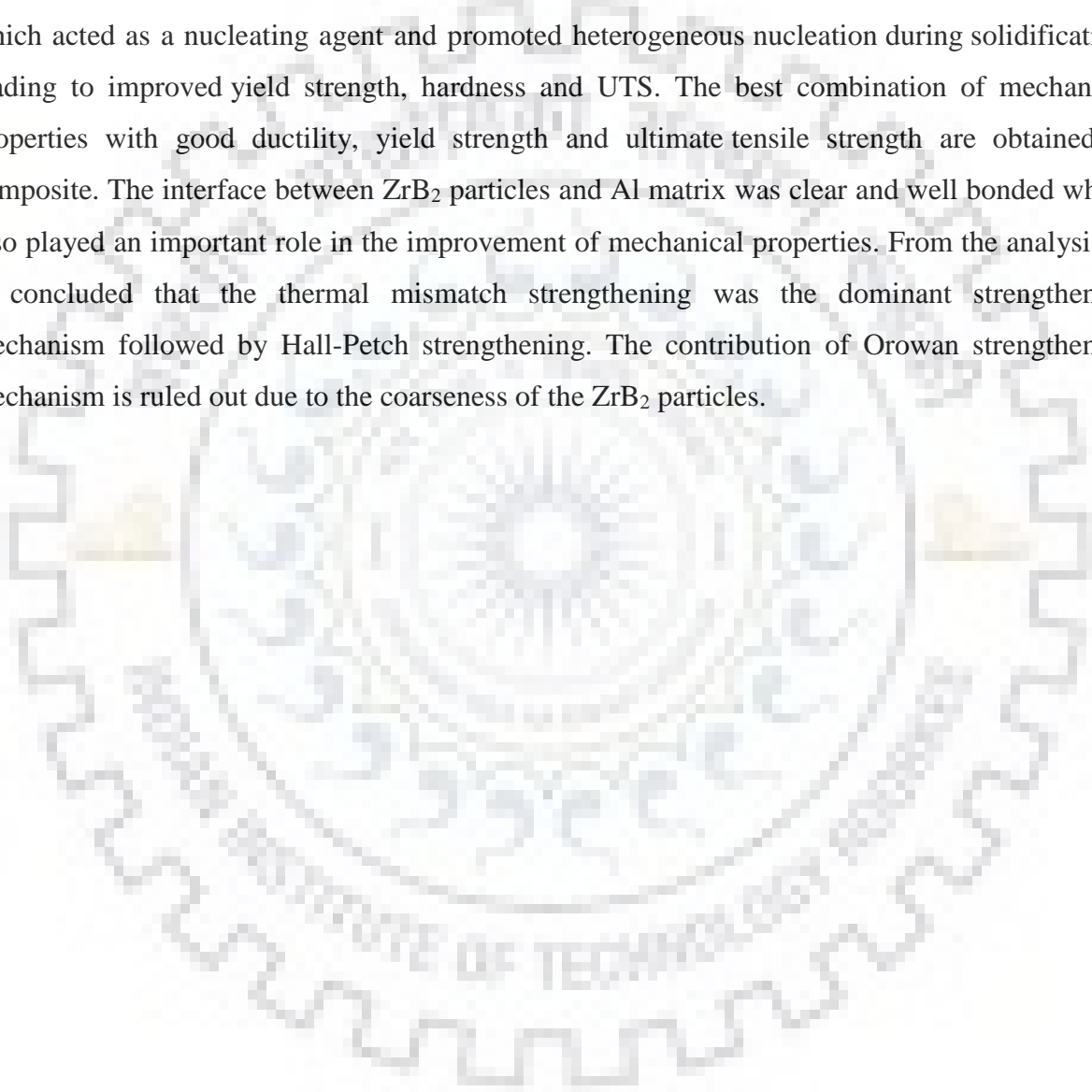


**Fig 15. SEM micrograph of the fracture surface of tensile specimens (a) base Al alloy; (b) 3wt% ZrB<sub>2</sub> (c) 6 wt% ZrB<sub>2</sub>.(d) 6 wt% ZrB<sub>2</sub> ultrasonication.**

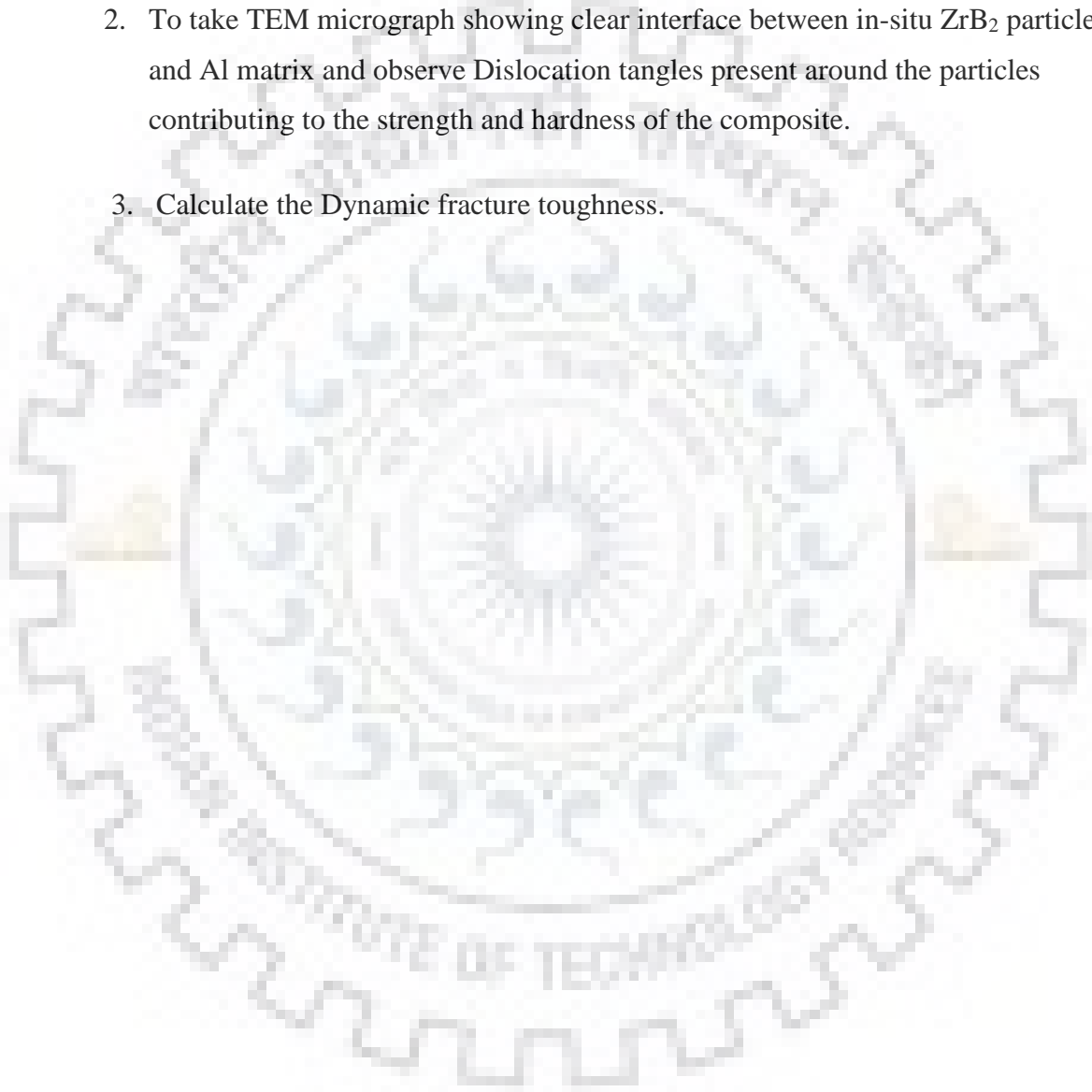
## **6. Conclusion**

Different amounts of  $K_2ZrF_6$  and  $KBF_4$  powder was reacted with 6061 aluminium alloy at  $850\text{ }^\circ\text{C}$  for 5 min to form in-situ  $ZrB_2$  particles under ultrasonication to achieve better dispersion of intermetallic. All  $ZrB_2$  particles were observed within the grains instead of segregation at grain boundaries. The grain size of the composites decreased due to the presence of particles which acted as a nucleating agent and promoted heterogeneous nucleation during solidification, leading to improved yield strength, hardness and UTS. The best combination of mechanical properties with good ductility, yield strength and ultimate tensile strength are obtained in composite. The interface between  $ZrB_2$  particles and Al matrix was clear and well bonded which also played an important role in the improvement of mechanical properties. From the analysis, it is concluded that the thermal mismatch strengthening was the dominant strengthening mechanism followed by Hall-Petch strengthening. The contribution of Orowan strengthening mechanism is ruled out due to the coarseness of the  $ZrB_2$  particles.



## **6.1 Scope for Future Work**

1. To calculate grain sizes of the composites formed and compare.
2. To take TEM micrograph showing clear interface between in-situ  $ZrB_2$  particles and Al matrix and observe Dislocation tangles present around the particles contributing to the strength and hardness of the composite.
3. Calculate the Dynamic fracture toughness.





## **6.2 References**

- [1] Qi Gao, Shusen Wu, Shulin Lü, Xinchun Xiong, Ping An.  
Effects of ultrasonic vibration treatment on particles distribution of TiB<sub>2</sub> particles reinforced aluminium composites.  
Research article Materials Science and Engineering: A Volume 680, 5 January 2017, Pages 437-443.
- [2] Qi Gao, Shusen Wu, Shulin Lü, Xinchun Xiong, Ping An.  
Improvement of particles distribution of in-situ 5 vol% TiB<sub>2</sub> particulates reinforced Al-4.5Cu alloy matrix composites with ultrasonic vibration treatment.  
Research article Journal of Alloys and Compounds, Volume 692, 25 January 2017, Pages 1-9
- [3] Muralidharan, K. Chockalingam, I. Dinaharan, K. Kalaiselvan.  
Microstructure and mechanical behavior of AA2024 aluminum matrix composites reinforced with in situ synthesized ZrB<sub>2</sub> particles.  
Research article Journal of Alloys and Compounds, Volume 735, 25 February 2018, Pages 2167-2174N.
- [4] .Microstructure and mechanical properties characterization of AA6061/TiC aluminum matrix composites synthesized by in situ reaction of silicon carbide and potassium fluotitanate.  
Research article Transactions of Nonferrous Metals Society of China, Volume 26, Issue 7, July 2016, Pages 1791-1800.
- [5] Mohanavel, M. Naveen Kumar, K. Mageshkumar, C. Jayasekar, S. Udishkumar..  
Mechanical behavior of in situ ZrB<sub>2</sub>/AA2014 composite produced by the exothermic salt-metal reaction technique.

Research article *Materials Today: Proceedings*, Volume 4, Issue 2, Part A, 2017, Pages 3215-3221V.

[6] Basiri Tochaee, H. R. Madaah Hosseini, S. M. Seyed Reihani.

On the fracture toughness behavior of in-situ Al-Ti composites produced via mechanical alloying and hot extrusion.

Research article *Journal of Alloys and Compounds*, Volume 681, 5 October 2016, Pages 12-21E.

[7] Rahul Gupta, G. P. Chaudhari, B. S. S. Daniel.

Strengthening mechanisms in ultrasonically processed aluminium matrix composite with in-situ  $Al_3Ti$  by salt addition.

Research article *composites Part B: Engineering*, Volume 140, 1 May 2018, Pages 27-34

[8] Riesch, J. -Y. Buffiere, T. Höschel, M. Scheel, J. -H. You.

Crack bridging in as-fabricated and embrittled tungsten single fibre-reinforced tungsten composites shown by a novel in-situ high energy synchrotron tomography bending test.

Research article *Nuclear Materials and Energy*, Volume 15, May 2018, Pages 1-12J.

[9] Xi Gao, Menghao Chen, Xiaogang Yang, Lee Harper, Jiawa Lu.

Simulating damage onset and evolution in fully bio-resorbable composite under three-point bending.

Research article *Journal*, Volume 81, May 2018, Pages 72-82

[10] J. Lapin, M. Štamborská, T. Pelachová, O. Bajana.

Fracture behaviour of cast in-situ TiAl matrix composite reinforced with carbide particles.

Research article *Materials Science and Engineering: A*, Volume 721, 4 April 2018, Pages 1-7

- [11] Gang Kou, Ling-jun Guo, Zhao-qian Li, Jian Peng, and Cai-xia Huo.  
Microstructure and flexural properties of C/C-Cu composites strengthened with in-situ grown carbon nanotubes.  
Research article *Journal of Alloys and Compounds*, Volume 694, 15 February 2017, Pages 1054-1060



